

P-Stereogenic Ir-MaxPHOX: A Step toward Privileged Catalysts for Asymmetric Hydrogenation of Nonchelating Olefins

Maria Biosca, Pol de la Cruz-Sánchez, Jorge Faiges, Jèssica Margalef, Ernest Salomó, Antoni Riera, Xavier Verdaguer,* Joan Ferré, Feliu Maseras, Maria Besora,* Oscar Pàmies, and Montserrat Diéguez*



Cite This: *ACS Catal.* 2023, 13, 3020–3035



Read Online

ACCESS |



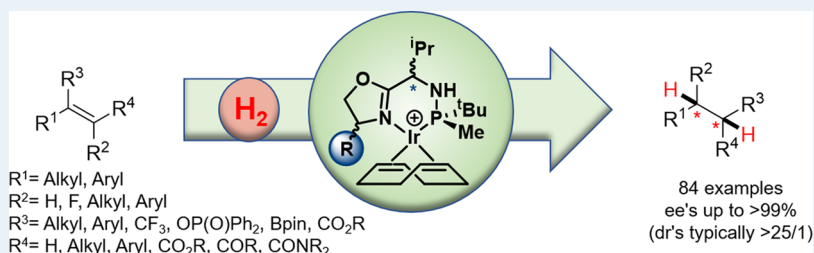
Metrics & More



Article Recommendations



Supporting Information



ABSTRACT: The Ir-MaxPHOX-type catalysts demonstrated high catalytic performance in the hydrogenation of a wide range of nonchelating olefins with different geometries, substitution patterns, and degrees of functionalization. These air-stable and readily available catalysts have been successfully applied in the asymmetric hydrogenation of di-, tri-, and tetrasubstituted olefins (ee's up to 99%). The combination of theoretical calculations and deuterium labeling experiments led to the uncovering of the factors responsible for the enantioselectivity observed in the reaction, allowing the rationalization of the most suitable substrates for these Ir-catalysts.

KEYWORDS: asymmetric hydrogenation, iridium, P–N ligands, DFT calculations, olefins

INTRODUCTION

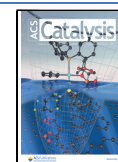
Advances in the synthesis of chiral molecules, whether creating new compounds or improving existing synthetic procedures, are made possible by the continuous innovations in asymmetric catalysis.¹ Among the asymmetric catalytic reactions that lead to enantiomerically pure products, the hydrogenation of olefins is one of the most powerful.^{1,2} This 100% atom economy process has a large record of successful examples in the production of single enantiomer intermediates, especially in the pharmaceutical industry, using substrates ranging from olefins with coordinating functional groups to nonfunctionalized counterparts, passing through olefins with intermediate coordinating properties.³ As the number of substrates continues to increase to reach more complex molecules, finding a catalyst that performs well with many of them regardless of geometry, substitution patterns, and functionalization remains a challenge. While Rh- and Ru-catalysts (mainly with diphosphine ligands) have been shown to be optimal for the reduction of olefins with strong coordinating functional groups,⁴ the Ir–P,X-catalysts (X = N, S, and O; mainly with phosphine/phosphinite/phosphite-oxazoline ligands) gave the best results for the hydrogenation of nonchelating alkenes.⁵ Particularly, the reduction of nonchelating olefins is the most difficult and less explored field since they do not have a coordinating group to help transfer the chiral information to the product. Currently, Ir-

catalysts only perform well for specific types of olefins. The most common substitution patterns are *E*-trisubstituted alkenes and, to a lesser extent, *Z*-trisubstituted and 1,1-disubstituted alkenes. The hydrogenation of tetrasubstituted olefins is the least developed category.⁵ Even for the most studied trisubstituted olefins, there is still room for improvement. For example, the reduction of the so-called purely alkyl-trisubstituted olefins, those without functional groups or aryl substituents, has been achieved in very few cases⁶ and the effectiveness for exocyclic substrates needs to be improved.⁷ For tetrasubstituted olefins, only a few specific Ir-catalysts have provided high performance for certain substrates, with variable enantioselectivity and low functional group tolerance. Most of the substrates studied were restricted to cyclic olefins and only a few were acyclic, mainly trimethyl styrene derivatives,^{7b,8} until recently when Gosselin's group in collaboration with Bigler, Pfaltz, and Denmark⁹ presented the reduction of a wide range of acyclic olefins with two or more aryl substituents. In addition, there are fewer reports of tetrasubstituted olefins with

Received: November 14, 2022

Revised: January 17, 2023

Published: February 14, 2023



poorly coordinative groups that are useful for further synthesis, and, in most cases, the same catalyst was unsuccessful for tetrasubstituted olefins without a poorly coordinative group.¹⁰ The finding of a catalyst that could work on all of them is highly desirable to limit time-consuming catalyst design and avoid a variety of preparation methods.

The bottleneck in finding the best catalysts is the identification of the right ligands with a broad substrate scope.¹¹ To overcome the substrate scope limitation in the asymmetric hydrogenation of nonchelating olefins, we recently reported on the first P,N-ligand library that could reduce different types of nonchelating olefins.^{7b} From a common backbone, the selection of the phosphite or phosphinite group led to ligands that were suitable for 56 examples of di-, tri-, and tetrasubstituted olefins. However, only 11 examples of tetrasubstituted olefins could be reduced, mainly indene derivatives and some acyclic olefins, to the detriment of tetrasubstituted acyclic alkenes with relevant poorly coordinative groups. Even for trisubstituted olefins, only one example of *Z*-olefin was successfully reduced and none of purely alkyl-substituted. Later on, we reported the successful application of a family of P-stereogenic aminophosphine-oxazoline (MaxPHOX) ligands in the Ir-catalyzed hydrogenation of the aforementioned unfunctionalized tetrasubstituted olefins and also in the reduction of several tetrasubstituted substrates with poorly coordinative groups, such as acyclic-tetrasubstituted vinyl fluorides with ester functionalities.^{8c}

To advance the search for a ligand library capable of hydrogenating a larger range of substituted nonchelating olefins, here we report an extension of the scope of olefins that Ir-MaxPHOX-type catalysts can successfully reduce. With the Ir-MaxPHOX 1-4a-c family of catalysts (Figure 1), we have

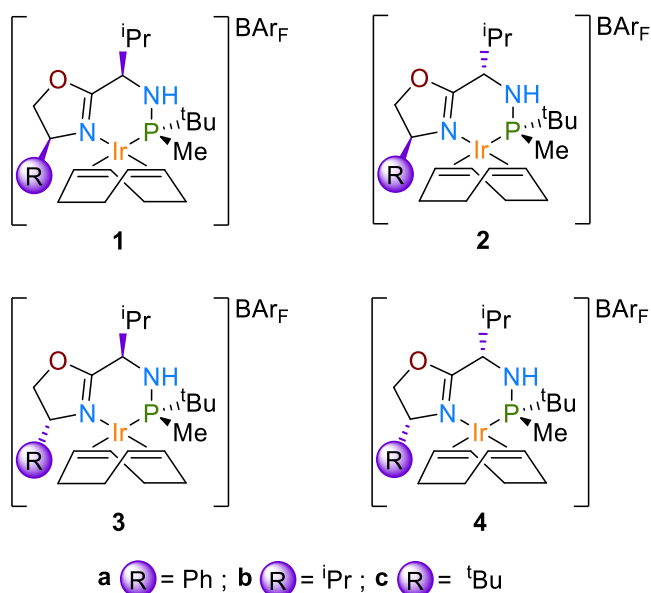


Figure 1. Family of aminophosphine-oxazoline iridium(I) catalysts (Ir-MaxPHOX) 1-4a-c.

been able to hydrogenate, with high catalytic performance, a wide range of di- and trisubstituted olefins and we have also increased the number of tetrasubstituted olefins containing neighboring poorly coordinative polar groups that could be used successfully. These catalysts have the advantage that they are prepared in four steps from available starting materials¹²

and allow us to easily study the effect of varying some ligand properties, such as the bulkiness of the oxazoline and its configuration and the configuration of the stereogenic center at the alkyl backbone chain. Together with mechanistic studies based on density functional theory (DFT) calculations and deuterogenation experiments, we were able to explain the origin of enantioselectivity, identify the preferred pathway, and predict enantioselectivities with good accuracy.

RESULTS AND DISCUSSION

Initial Catalytic Screening. As mentioned in the introduction, the hydrogenation of nonchelating olefins depends largely on the substitution pattern of the substrate. The most successful examples have been reported for *E*-trisubstituted, while 1,1'-disubstituted olefins are usually hydrogenated less enantioselectively and tetrasubstituted olefins are still underdeveloped.⁵ To explore the scope of the Ir-MaxPHOX catalysts (1-4a-c), we initially applied them in the asymmetric hydrogenation of the nonfunctionalized disubstituted olefin **S1** and the widely used benchmark trisubstituted substrate **S2** (Table 1). The initial test

Table 1. Asymmetric Hydrogenation of Substrates **S1**, **S2**, and **S3**^{8c} with Ir-Catalysts 1-4a-c^a

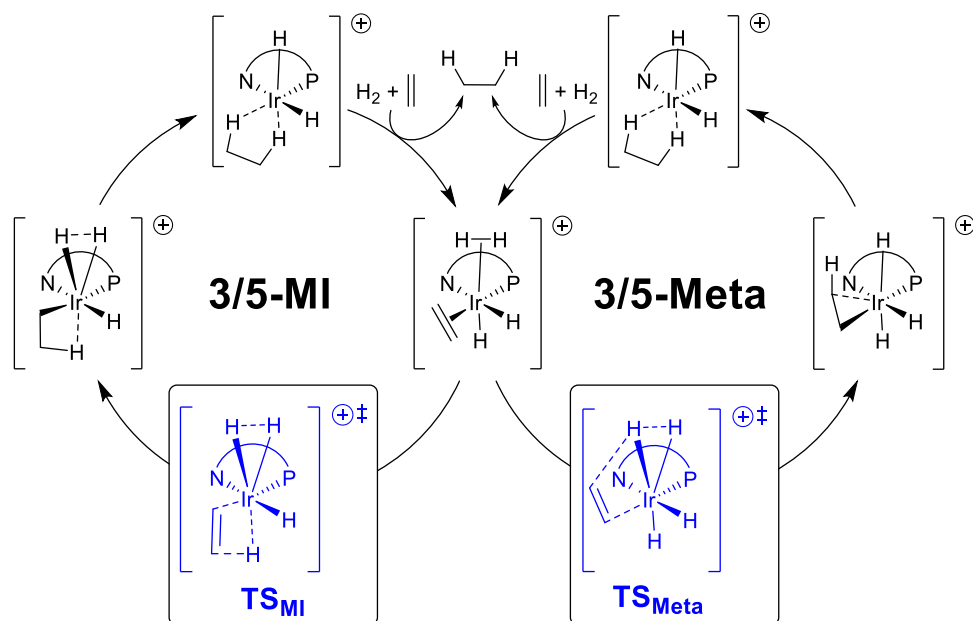
entry	Ir complex	% conv ^b	% ee ^c	% conv ^b	% ee ^c	% conv ^b	% ee ^c
1	1a	100	74 (S)	100	67 (R)	100	75 (R)
2	1b	100	66 (S)	100	75 (R)	100	85 (S) ^d
3	1c	100	81 (S)	100	77 (R)	85	44 (R)
4	2b	100	15 (S)	100	15 (S)	85	33 (S)
5	3b	100	80 (R)	100	23 (S)	100	44 (R)
6	4a	100	83 (R)	100	82 (S)	100	28 (R)
7	4b	100	88 (R)	100	85 (S)	100	25 (R)
8	4c	100	91 (R)	100	88 (S)	100	31 (R)
9 ^e	4c	100	91 (R)	100	89 (S)		
10 ^e	1b					100	98 (S) ^f

^aReaction conditions: catalyst (1 mol %), CH₂Cl₂, 1 bar of H₂ (**S1**), 50 bar of H₂ (**S2**), or 75 bar of H₂ (**S3**), rt, 4 h (**S1** and **S2**) or 24 h (**S3**). ^bConversions were measured by ¹H NMR spectroscopy after 4 h (**S1** and **S2**) or 24 h (**S3**). ^cEnantiomeric excess determined by GC. ^dUsing 2 bar of H₂—98% (S) ee. ^eReactions carried out in PC instead of CH₂Cl₂ after 6 h (**S1** and **S2**) and 30 h (**S3**). ^fUsing 2 bar of H₂.

conditions were the optimal conditions reported in previous studies with other P,N ligands.⁵ Therefore, the reactions were carried out at room temperature using 1 mol % of the catalyst in dichloromethane under 1 bar of H₂ for the disubstituted substrate **S1** and 50 bar of H₂ for the trisubstituted olefin **S2**. The previous results for the model acyclic-tetrasubstituted substrate **S3** were also included in Table 1 for comparison.^{8c}

For substrates **S1** and **S2**, the best enantioselectivities were obtained with Ir-catalyst **4c** (ee's up to 91%, entry 8) regardless of the substitution pattern of the substrate. The results showed that both the oxazoline substituent and the diastereoisomeric backbone of the ligand had a noticeable effect on the stereochemical outcome. This effect also occurred in the hydrogenation of the tetrasubstituted olefin **S3**. However, while for the di- and trisubstituted substrates (**S1** and **S2**) the best results were obtained with the bulkier ^tBu

Scheme 1. Proposed Catalytic Cycles 3/5-MI and 3/5-Meta for the Asymmetric Hydrogenation of Nonchelating Olefins



group in the oxazoline (e.g., see entry 8 vs. 6–7), the best results for the tetrasubstituted substrate **S3** were obtained with the less bulky ⁱPr group, in accordance with the higher steric hindrance of **S3** (entry 2). Similarly, the effect of the diastereoisomeric backbone differed between the di/trisubstituted alkenes **S1** and **S2** and the tetrasubstituted olefin **S3**. While backbone **4** (Figure 1) was best for **S1** and **S2** (ee's up to 91%), the best backbone for **S3** was **1** (ee's up to 98% at 2 bars of H₂, entry 2). In summary, optimizing the ligand structure led us to identify **1b** and **4c** as the best catalysts of the family for the hydrogenation of olefins with different substitution patterns.¹³

To make the process more sustainable, the reaction was carried out in 1,2-propylene carbonate (PC),¹⁴ an eco-friendly alternative to standard organic solvents due to its high boiling point, low toxicity, and green synthesis (Table 1, entries 9 and 10). Advantageously, enantioselectivities remained as high as those obtained with dichloromethane (ee's up to 98%). In addition, the catalyst could be recycled up to five times with a simple two-phase extraction with hexane with a minimal decrease in enantioselectivity (see the Supporting Information).

Mechanistic Studies: The Origin of Enantioselectivity.

To understand why the best ligand for tetrasubstituted olefins is different from that of di- and trisubstituted analogues, we performed a density functional theory (DFT) study. The transition states (TSs) involved in the enantiodetermining step of the reaction for the tri- and tetrasubstituted olefins, **S2** and **S3**, with catalyst **4c** (for **S2**) and catalysts **1b** and **4c** (for **S3**) were searched using the B3LYP¹⁵ functional with the Grimme Dispersion correction, GD3.¹⁶ Mechanistically it is well known that Ir-catalyzed hydrogenation of nonfunctionalized alkenes proceeds through an Ir(III)/Ir(V) tetrahydride intermediate¹⁷ and enantioselectivity is determined in the first hydrogen transfer from the metal to the coordinated olefin. Our calculations also support this mechanism; the free energy reaction profile is presented in the Supporting Information. Consequently, enantioselectivity can be reliably estimated from the relative energies of the TSs of this step. Nevertheless, two

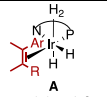
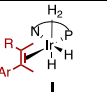
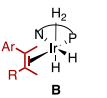
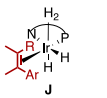
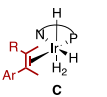
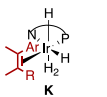
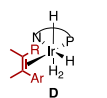
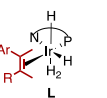
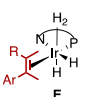
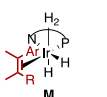
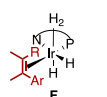
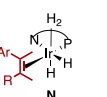
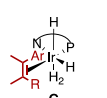
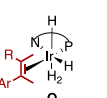
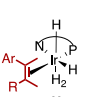
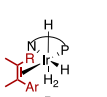
different mechanisms can be considered for this process: (i) an Ir(III)/Ir(V) migratory-insertion step (mechanism 3/5-MI, Scheme 1) and (ii) an Ir(III)/Ir(V) σ -bond metathesis (mechanism 3/5-Meta, Scheme 1). While (i) is usually the most favorable mechanism, (ii) is also energetically feasible and cannot be immediately discarded. We, therefore, computed the TSs for both pathways (see the Supporting Information for the full set of calculated TSs). A data set collection of computational results is available in the ioChem-BD repository.¹⁸

The calculated relative energies for the most stable isomers of the TSs for both pathways (TS_{Mi} and TS_{Meta}) are shown in Table 2. These key isomers are the result of the relative arrangement of the hydride (up or down), the coordination of the olefin through the *Re*- or *Si*-face, and the attack of the hydride through the two olefinic carbons (C₁ or C₂). In addition, in these calculations, we also considered the rotamers of the isopropyl group. As in other reported studies, the results show that in all cases, the migratory insertion is the preferred reaction pathway.

Positively, the calculations for the trisubstituted substrate **S2** with the Ir-catalyst **4c** reproduce the experimental outcome. The favored pathway TS_L (Table 2) proceeds through the *Re*-face, which leads to the formation of the (*S*)-product, and the energy difference between the two most stable TSs (TS_L and TS_O, Table 2), which lead to opposite enantiomers, is 5.3 kJ/mol (ee_{calc} = 79% (*S*)) in agreement with the experimental enantioselectivity (88% (*S*)). Single-point calculations on the most stable TSs with larger basis sets, B97D3/cc-pVTZ & cc-pVTZ-PP, improve the agreement ee_{calc} = 85% (*S*) (see the Supporting Information for further details). Thus, the factors responsible for enantioselectivity can be deduced by analyzing the structures of both TSs via quantitative quadrant diagram representations using MolQuO¹⁹ software (Figure 2).

Figure 2a shows the quadrant diagram obtained by analyzing the two most stable TSs for the hydrogenation of **S2** (TS_L and TS_O, Table 2).²⁰ In this diagram, the oxazoline substituent (^tBu) blocks the lower-left quadrant Q3 (quadrant occupancy = 3.8), while the methylenic carbon of the oxazoline partly

Table 2. Calculated Relative Energies (kJ/mol) for the Transition States TS_{MI} and TS_{Meta} with Substrates **S2** and **S3** Using Ir-Catalyst **4c** (for **S2**) and Ir-Catalysts **1b** and **4c** (for **S3**)^{a,b}

TS_{Meta}	4c/S2	4c/S3	1b/S3	TS_{MI}	4c/S2	4c/S3	1b/S3
 A attack through C ₁ Si-face coordination	56.7	35.7	17.3	 I attack through C ₁ Si-face coordination	39.3	37.8	8.5
 B attack through C ₁ Re-face coordination	18.3	25.1	7.3	 J attack through C ₁ Re-face coordination	60.3	49.7	21.3
 C attack through C ₁ Si-face coordination	20.1	12.9	15.7	 K attack through C ₁ Si-face coordination	26.3	7.3	27.0
 D attack through C ₁ Re-face coordination	34.3	19.1	27.7	 L attack through C ₁ Re-face coordination	0.0	10.7	24.9
 E attack through C ₂ Si-face coordination	44.6	39.7	11.1	 M attack through C ₂ Si-face coordination	61.7	37.2	4.4
 F attack through C ₂ Re-face coordination	55.1	36.9	13.9	 N attack through C ₂ Re-face coordination	19.1	28.3	0.0
 G attack through C ₂ Si-face coordination	38.9	15.5	29.2	 O attack through C ₂ Si-face coordination	5.3	0.0	17.0
 H attack through C ₂ Re-face coordination	5.6	9.9	24.8	 P attack through C ₂ Re-face coordination	32.6	6.4	28.7

^aValues in blue and bold indicate the lowest *Re* and *Si* energy TSs for each combination of substrate and catalyst. ^bRelative Gibbs free energies (kJ/mol) in solution (B3LYP-D3/6-31G(d,p)&LANL2DZ) with respect to the corresponding lowest energy transition state; for **S2** Ar = 4-CH₃O-C₆H₄ and R = H and for **S3** Ar = C₆H₅ and R = CH₃; C₁ is the least electronegative olefinic carbon atom and C₂ is the most electronegative one. In all TSs, the most stable rotamer was selected.

occupies the upper-left quadrant Q1 (quadrant occupancy = 1.6) making it semihindered (Figure 2a). The other two quadrants, Q2 and Q4, free from bulky groups, are empty (quadrant occupancy = 0). According to this model, the coordination of the trisubstituted olefin **S2** through the *Re*-face is favored because the smallest substituent, the olefinic hydrogen, is located in the most hindered quadrant Q3 and the aryl substituent (4-OMe-C₆H₅) is located in the semi-hindered quadrant Q1 (Figure 2b). In contrast, when the olefin coordinates through the *Si*-face, which leads to the opposite enantiomer ((*R*)-enantiomer, TS_O , Table 2), the aryl group is located at the most hindered quadrant resulting in a less favorable TS (Figure 2c). The occupancy value for this quadrant (3.1) is slightly lower than that obtained for the TS leading to the major product, indicating that the ligand adapts

its chiral pocket to suit the olefin in this coordination manner. It is noteworthy that all TSs with the methyl group located in Q3 are less stable, at least 26.3 kJ/mol higher in energy than the most stable one. Note that despite the small size of a methyl group, the flat 4-MeO-C₆H₅ group fits better into the cavity in Q3. In summary, the model indicates that the stereochemical outcome with trisubstituted olefin **S2** depends on steric factors. Following this observation, it can be hypothesized that the catalyst may also work for other aryl-containing trisubstituted olefins, including the less studied triaryl trisubstituted and *Z*-olefins (see Table 3 below), where the TS with olefinic hydrogen located in the most hindered quadrant Q3 will continue to be more stable than a TS with the aryl substituent (for triaryl olefins) or the methyl substituent (for *Z*-olefins) in Q3. In addition, this model

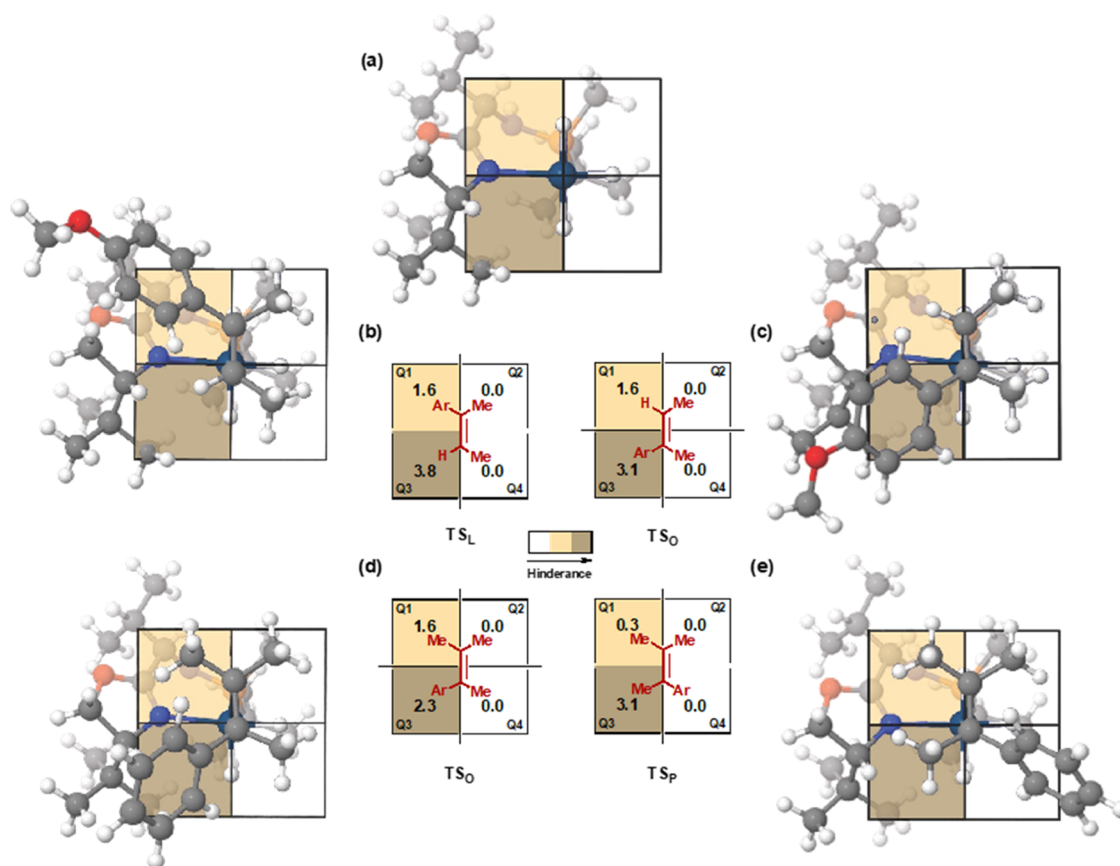


Figure 2. Models of the most favored TSs for the asymmetric hydrogenation of **S2** and **S3** with **4c**; (a) schematic quadrant model for **4c** (the olefin coordinates above the plane of the paper), (b) the most favorable coordination of **S2** giving the major (*S*)-product, (c) the most favorable coordination of **S2** giving the minor (*R*)-product, (d) the most favorable coordination of **S3** giving the major (*R*)-product, and (e) the most favorable coordination of **S3** giving the minor (*S*)-product.

suggests that if the olefinic aryl group is replaced by a bulkier substituent (e.g., purely alkyl-substituted olefins), then a higher destabilization of the TS_O could be expected, resulting in a higher energy gap between the TSs and high enantioselectivity (see results for **S20** and **S21**, Table 3 below).

In contrast, the most favorable TS with the same Ir-catalyst **4c** system but with the tetrasubstituted olefin **S3** was TS_O (Table 2), where the olefin coordinates through the *Si*-face and the (*R*)-enantiomer would be obtained as observed experimentally. The quadrant diagrams of the two most stable TSs (TS_O and TS_P, Table 2) with the tetrasubstituted olefin **S3** and **4c** were analyzed (Figure 2d,e). The diagrams show that the preferred coordination of **S3** is through the *Si*-face with the olefinic phenyl substituent occupying the most hindered quadrant (Q3, Figure 2d), which explains why the enantioselectivity is opposite to that of **S2**. Again, the planarity of the phenyl substituent makes the TS less crowded in Q3 than with a methyl group. This is reflected in the fact that the distance between the hydrogen of the C₄ of the oxazoline and the olefinic phenyl substituent (TS_O) is greater than the distance between the hydrogen of the C₄ of the oxazoline and the methyl substituent in the TS_P (Figure 3).

When Ir-catalyst **1b** was used in the hydrogenation of tetrasubstituted olefin **S3**, reverse enantioselectivity was obtained compared to Ir-catalyst **4c**. This can be rationalized by analyzing the quadrant model of the most stable transition state, TS_N (Table 2), for the hydrogenation of **S3** with **1b** (Figure 4). Ir-catalyst **1b** has the opposite configuration in the

oxazoline substituent compared to **4c**, making the upper-left quadrant Q1 the most hindered (Figure 4a). Therefore, the preferred coordination of **S3** is through the *Re*-face (the opposite of **4c**) with the olefinic phenyl located in the most hindered quadrant (Q1) (Figure 4b).

Although the sense of enantioselectivity for **S3** was well predicted for both Ir-catalysts **4c** and **1b**, the enantioselectivity value was greatly overestimated with **4c** (82% (*R*) B3LYP-D3/6-31G(d,p)&LANL2DZ and 85% (*R*) B97D3/cc-pVTZ&cc-pVTZ-PP//B3LYP-D3/6-31G(d,p)&LANL2DZ predicted ee vs. 31% (*R*) observed ee). To explain this disagreement, we conducted deuterium labeling experiments with **1b** and **4c** (Scheme 2) in which the related tetrasubstituted olefin **S4** was reduced with deuterium. Note that in these deuterogenation experiments, we used substrate **S4**, which differs from the tetrasubstituted olefin **S3** in a methoxy group in the aryl group, which was introduced to facilitate product analysis. Both substrates performed in the same way. As expected, no deuteration at the methyl groups was observed using **1b**. However, in the case of **4c**, a substantial deuteration was found at the allylic position, indicating the existence of a competing isomerization process. This isomerization would explain the lower enantioselectivity observed when using **4c** in the hydrogenation of tetrasubstituted alkenes such as **S3** or **S4** (Table 1, entry 2 vs. 7).

Substrate Scope. We first evaluated the Ir-precatalysts **1a-c** in the reduction of a wide range of di- and trisubstituted

Table 3. Asymmetric Hydrogenation of Nonfunctionalized Trisubstituted Olefins with Only Aryl and/or Alkyl Substituents S5–S30

Entry	Substrate	% Conv	% ee	Entry	Substrate	% Conv	% ee
1		100	90 (<i>R</i>)	12		100	83 (<i>R</i>)
2		100	94 (<i>R</i>)	13		100	91 (<i>R</i>)
3		100	92 (<i>R</i>)	14		100	87 (<i>R</i>)
4		100	92 (<i>R</i>)	15		100	99 (<i>R</i>)
5		100	92 (<i>R</i>)	16		100	98 (<i>R</i>)
6		100	94 (<i>R</i>)	17		100	>98 (<i>S</i>)
7		100	93 (<i>R</i>)	18		100	>98 (<i>S</i>)
8		100	80 (<i>R</i>) ^a	19		100	86 (<i>R</i>)
9		100	90 (<i>R</i>) ^b	20		100	84 (<i>R</i>)
10		100	94 (<i>S</i>)	21		100	85 (<i>R</i>)
11		100	93 (<i>S</i>)	22		100	83 (<i>R</i>)
				23		100	83 (<i>R</i>)
				24		100	81 (<i>R</i>)
				25		100	83 (<i>R</i>)
				26		100	83 (<i>R</i>)
				27		100	74 (<i>R</i>)

^aReaction conditions: **4c** (1 mol %), CH₂Cl₂, 23 °C, 4 h, using 1 bar of H₂ for **S5**–**S12** or 50 bar of H₂ for **S13**–**S30**. ^bReaction carried out using propylene carbonate (PC) as a solvent for 6 h.

substrates with *E*- and *Z*-geometries and different neighboring polar groups.

We first focused on the hydrogenation of nonfunctionalized olefins with aryl and/or alkyl substituents only (Table 3). According to the previous screening, Ir-catalyst **4c** was selected for the hydrogenation of a wide range of 1,1'-disubstituted olefins. As expected, this catalyst provided high enantioselectivities (up to 94% ee) for other α -*tert*-butylstyrenes (substrates **S5**–**S11**) with a range of electronic and steric properties at the aryl group. These are significant results because disubstituted substrates suffer more face-selectivity

indetermination than the trisubstituted equivalents and therefore there are fewer catalysts²¹ that can provide those high ee's. Nevertheless, the hydrogenation of α -alkylstyrene **S12**, which has a less bulky ethyl group, proceeded with lower enantioselectivity (ee' up to 80%) than α -*tert*-butylstyrenes. Although this is still a remarkable result for this challenging substrate, the lower ee was due to the isomerization of **S12** (as observed in deuteration experiments; see the Supporting Information). Thus, like the most successful cases reported in the literature,²² the competition between direct hydrogenation and isomerization is responsible for the observed decrease in

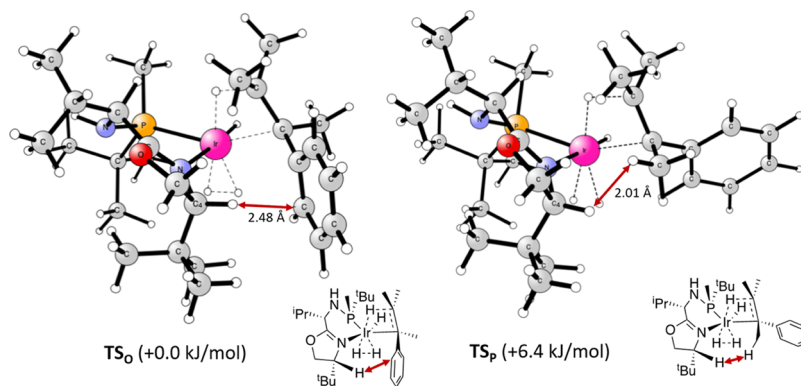


Figure 3. Representation of the two most stable TSs (TS₀ and TS_p) for **4c** and substrate **S3**. Relative Gibbs free energies in solution (kJ/mol) with respect to the corresponding lowest TS.

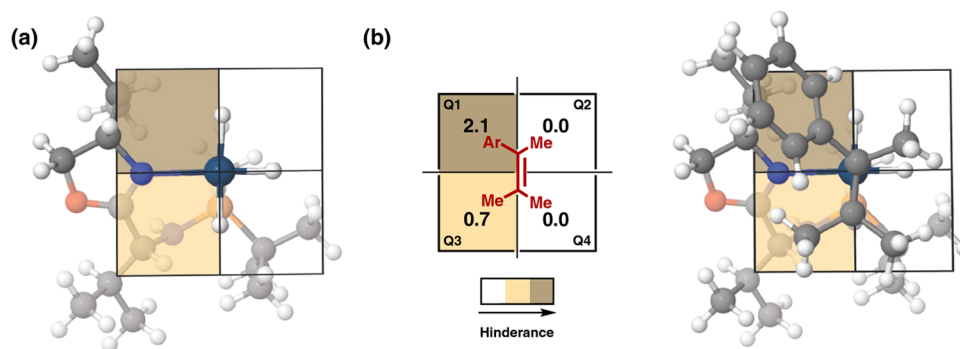
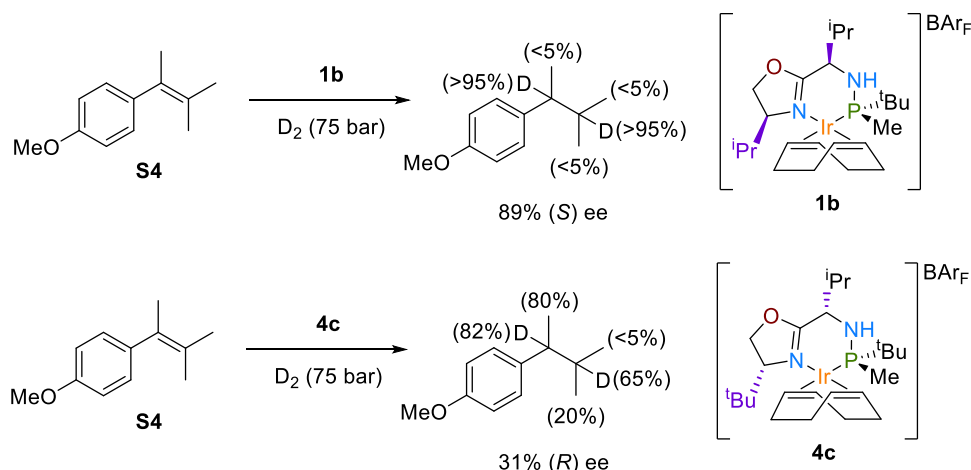


Figure 4. Model of the most favored TS for the asymmetric induction of **S3** with **1b**; (a) schematic quadrant model for **1b** (the olefin coordinates above the plane of the paper) and (b) the most favorable coordination of **S3** giving the major (*S*)-product.

Scheme 2. Deuterium Labeling Experiments of the Tetrasubstituted Substrate (**S4**)^a

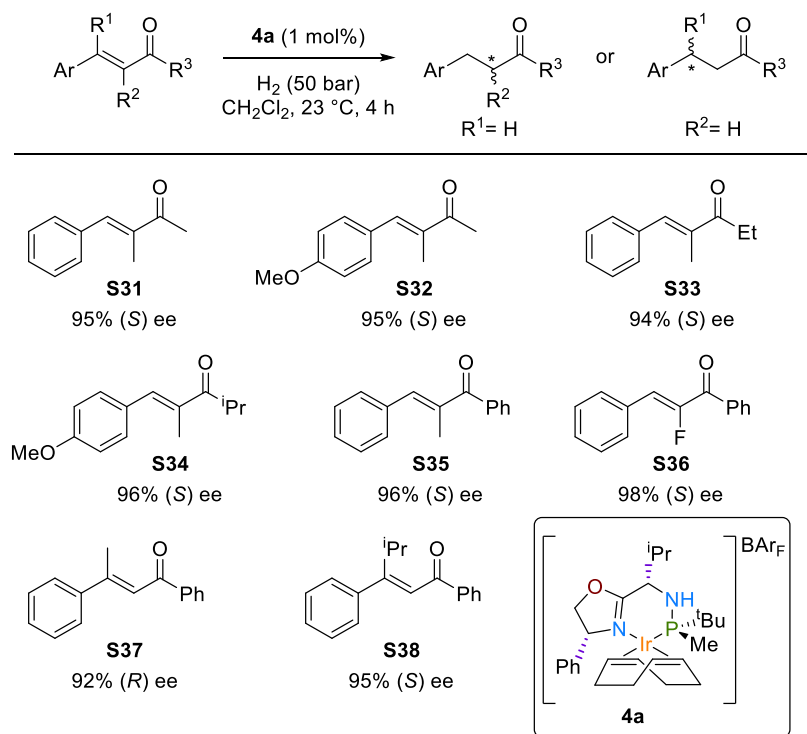


^aPercentage of deuterium incorporation is shown in brackets.

enantioselectivity. Börner et al. found that the use of 1,2-propylene carbonate (PC) as a solvent reduces the isomerization rate.^{14a} We, therefore, performed the reaction of **S12** in PC and we were glad to see that the enantioselectivity increased to 90% ee (entry 9).

As far as the hydrogenation of aryl trisubstituted olefins is concerned (**S13**–**S19**; Table 3, entries 10–16), the catalyst **4c** also worked well for those with an *E*-geometry, **S13** and **S14** (ee's up to 94%), which differ from **S2** in the substituent of the aryl ring and the substituent *trans* to the aryl group as well as for the more challenging *Z*-geometry alkenes **S15**–**S17** (ee's

up to 91%). In addition, the substrate scope was extended to the triaryl trisubstituted substrates **S18** and **S19** (ee's up to 99%), whose reduction has been less studied despite the fact that they are an easy entry point to obtain diaryl methane chiral centers present in natural products and medicines.²³ These catalytic results are completely consistent with the calculated TSs (vide supra). The analysis of the TSs indicated that the stereochemical outcome for the *E*-olefins mainly depends on steric factors. This finding suggested that enantioselectivities could also be high for substrates such as **S2** that have a bulkier group in the position of the phenyl moiety. This hypothesis

Scheme 3. Asymmetric Hydrogenation of α,β - and β,β -Unsaturated Trisubstituted Enones^a

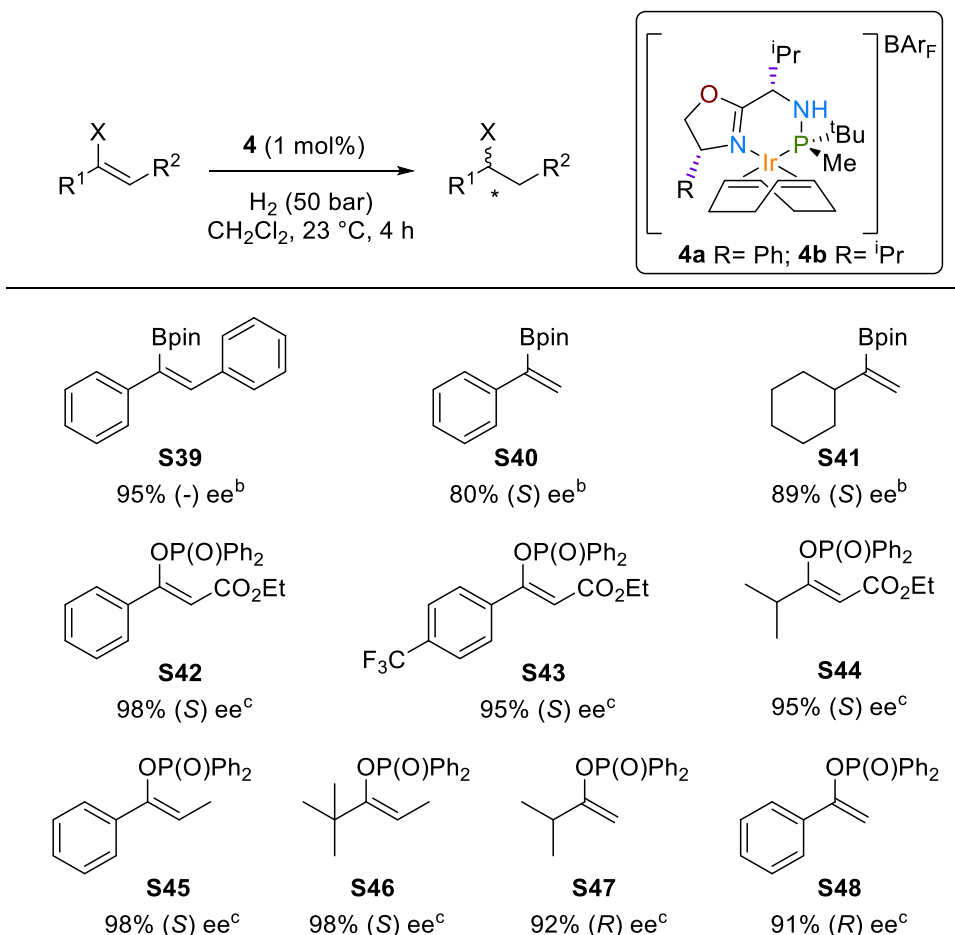
^aFull conversions were achieved in all cases.

was confirmed by the high enantioselectivities (ee's > 98%) found in the hydrogenation of substrates **S20** and **S21**, which contain a bulky isopropyl and cyclohexyl group, respectively (Table 3, entries 17 and 18).²⁴ These are valuable results because the highly enantioselective hydrogenation of purely alkyl substrates is rare,⁶ and indicate that the chiral pocket of the catalyst **4c** is suitable for achieving the hydrogenation of these elusive substrates with excellent enantiocontrol.

The results up to this point led us to test the reduction of exocyclic trisubstituted olefins (**S22**–**S30**, Table 3). The hydrogenation of these substrates is of interest because the chiral benzofused ring motif is present in pharmaceuticals, natural products, and intermediates of relevant bioactive drugs.²⁵ Despite the similarities with the acyclic olefins discussed above, the asymmetric hydrogenation of exocyclic olefins has hardly been explored and has yet to be resolved. The main challenge with exocyclic olefins is that the stereochemical outcome is highly influenced by ring size, and until recently, only a few examples had been able to provide high enantiocontrol, particularly for exocyclic olefins with a benzofused 5-membered ring^{7a,b,26} although enantioselectivity decreased when an *ortho*-substituent was present and required an additive to work.²⁷ Positively, the stereochemical outcome using Ir-catalyst **4c** was barely affected by the size of the ring of the substrate, being able to hydrogenate five- and six-membered ring benzofused olefins with high enantioselectivities (up to 86% ee, Table 3) at room temperature without additives. In addition, **4c** tolerates well the presence of several substituents that decorate the aryl group, even an *ortho* group. Note also that, surpassing the previously reported results, the more challenging benzofused olefin with a four-membered ring **S30** could also be hydrogenated with a significant enantioselectivity of 74% ee.

We then moved on to asymmetric hydrogenation of key acyclic olefins with neighboring polar groups. In this context, a set of α,β -unsaturated trisubstituted acyclic enones **S31**–**S36** (Scheme 3) could be hydrogenated with enantioselectivities comparable to the best ones reported but, in contrast to the asymmetric hydrogenation of di- and trisubstituted alkenes mentioned above, this was done with the catalytic system **4a**.^{7d–f,28} The reduction of these olefins opens a direct, atom-efficient path to prepare optically pure ketones, the synthesis of which until now has been mainly based on noncatalytic methods with a limited substrate scope. The attained enantioselectivities, between 95 and 98% ee, were quite independent of the nature of the substituents, which also allowed the successful hydrogenation of the highly appealing α -fluoride substituted enone **S36**.²⁹ It has been reported that the stereochemical outcome in the hydrogenation of acyclic enones is greatly influenced by the enone substitution pattern and, therefore, only a few catalysts have been able to hydrogenate both α,β - and β,β -unsaturated trisubstituted enones with high enantioselectivities.^{28c,d} Gratifyingly, the catalytic system **4a** also proved to be very efficient in the hydrogenation of β,β -unsaturated enones **S37** and **S38** (Scheme 3).

We then tested whether the high enantioselectivities were maintained for acyclic olefins containing other relevant neighboring polar groups (see Scheme 4, substrates **S39**–**S48**). High enantioselectivities up to 98% in alkenyl boronic esters and enol phosphinates were obtained. Among these results, one can highlight the effective hydrogenation of the pure alkyl-trisubstituted enol phosphinates **S44** and **S46**, a good alternative to the hydrogenation of dialkyl ketones to alcohols whose hydrogenation is still elusive. While for the reduction of vinyl boronate, the best enantioselectivity was achieved with **4b** (95% ee); for enol phosphinates, the highest

Scheme 4. Asymmetric Hydrogenation of Vinyl Boronates S39–S41 and Enol Phosphinates S42–S48^a

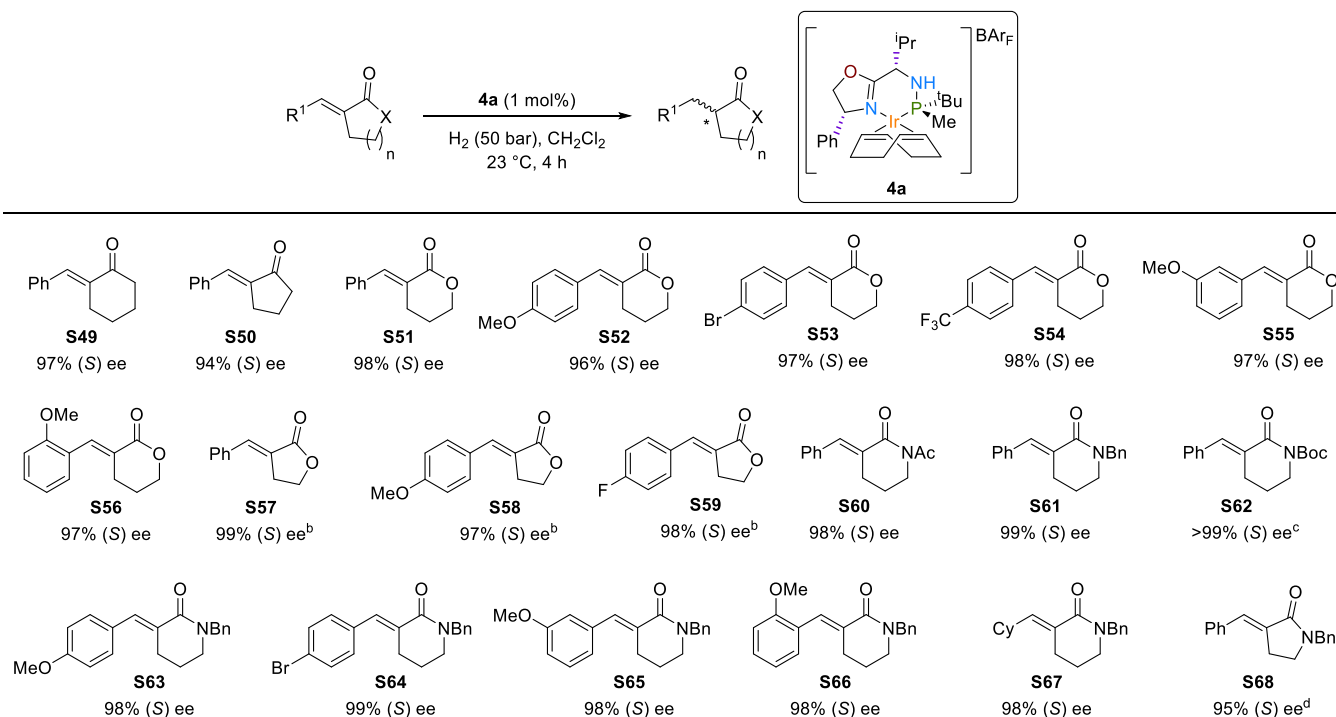
^aFull conversions were achieved in all cases. ^bReactions carried out using **4b**. ^cReactions carried out with **4a**.

enantioselectivities (up to 98% ee) were with **4a**. Both types of substrates are of interest because their reduction opens up straightforward routes for preparing enantiomerically pure organoboron and organophosphorus compounds, which can be easily transformed into high-value compounds.³⁰ The excellent enantioselectivities obtained in the hydrogenation of the trisubstituted alkenyl boronic ester and enol phosphinates were also reached in the even more challenging disubstituted analogues (**S40**, **S41** and **S47**, **S48**; up to 92% ee), including the hydrogenation of nonaromatic disubstituted olefins **S41** and **S47**.

Subsequently, we focused on the asymmetric hydrogenation of exocyclic olefins containing a neighboring polar group (Scheme 5, **S49**–**S68**). In particular, we considered the hydrogenation of α,α -unsaturated exocyclic enones and α,α -unsaturated lactones and lactams, since the reduced products of these olefins are encountered in natural products and drugs.³¹ These substrates suffer from the same ring size limitation that was discussed for exocyclic olefins without a neighboring polar group.⁷ In our case, however, the hydrogenation of the exocyclic enones **S49** and **S50** using **4a** proceeded with high enantioselectivities (up to 97%), comparable to the best ones, regardless of the size of the ring. In addition, hydrogenation of α,α -unsaturated lactones (**S51**–**S59**) also proceeded with excellent levels of enantioselectivity (ee's up to 99%) regardless of the size of the lactone ring. In addition, ee's were found to be quite independent of

the electronic and steric nature of the olefinic substituent. Chiral α -substituted- δ -valerolactones and γ -butyrolactones were therefore attained with ee's up to 99%. The hydrogenation of α,α -unsaturated lactams (**S60**–**S68**) followed the same trend as related lactones, with ee's up to >99%. Note that the Ir-catalyst **4a** also allows the presence of different protecting groups, such as Bn, Ac, and Boc, albeit in the latter case, the Boc group can also be partially cleaved under the reaction conditions.

Finally, we studied how using Ir-catalysts **1-4a-c**, we can extend the asymmetric hydrogenation domain to new types of tetrasubstituted olefins. Tetrasubstituted acyclic olefins are considered to be some of the most challenging substrates to be hydrogenated due to the difficulty in differentiating the prochiral faces and the slow activities that result from their steric hindrance. Compared to the progress made with functionalized tetrasubstituted olefins, the reduction of non-chelating tetrasubstituted acyclic olefins remains an open challenge. Furthermore, there are only a few reports on the hydrogenation of tetrasubstituted olefins with poorly coordinative groups that can create intermediates useful for subsequent synthesis.¹⁰ As mentioned in the Introduction section, the Ir-catalysts **1-4a-c** were successfully applied in reducing a range of nonchelating tetrasubstituted substrates, most of them without poorly coordinative groups. However, high enantioselectivities were attained in the reduction of several acyclic-tetrasubstituted vinyl fluorides containing an

Scheme 5. Asymmetric Hydrogenation of Exocyclic α,α -Unsaturated Enones, Lactones, and Lactams (S49–S68)^a

^aFull conversions were attained in all cases otherwise noted. ^bReactions carried out using 2 mol% of catalysts. ^c28% of deprotected lactam was also obtained. ^d76% conversion was attained.

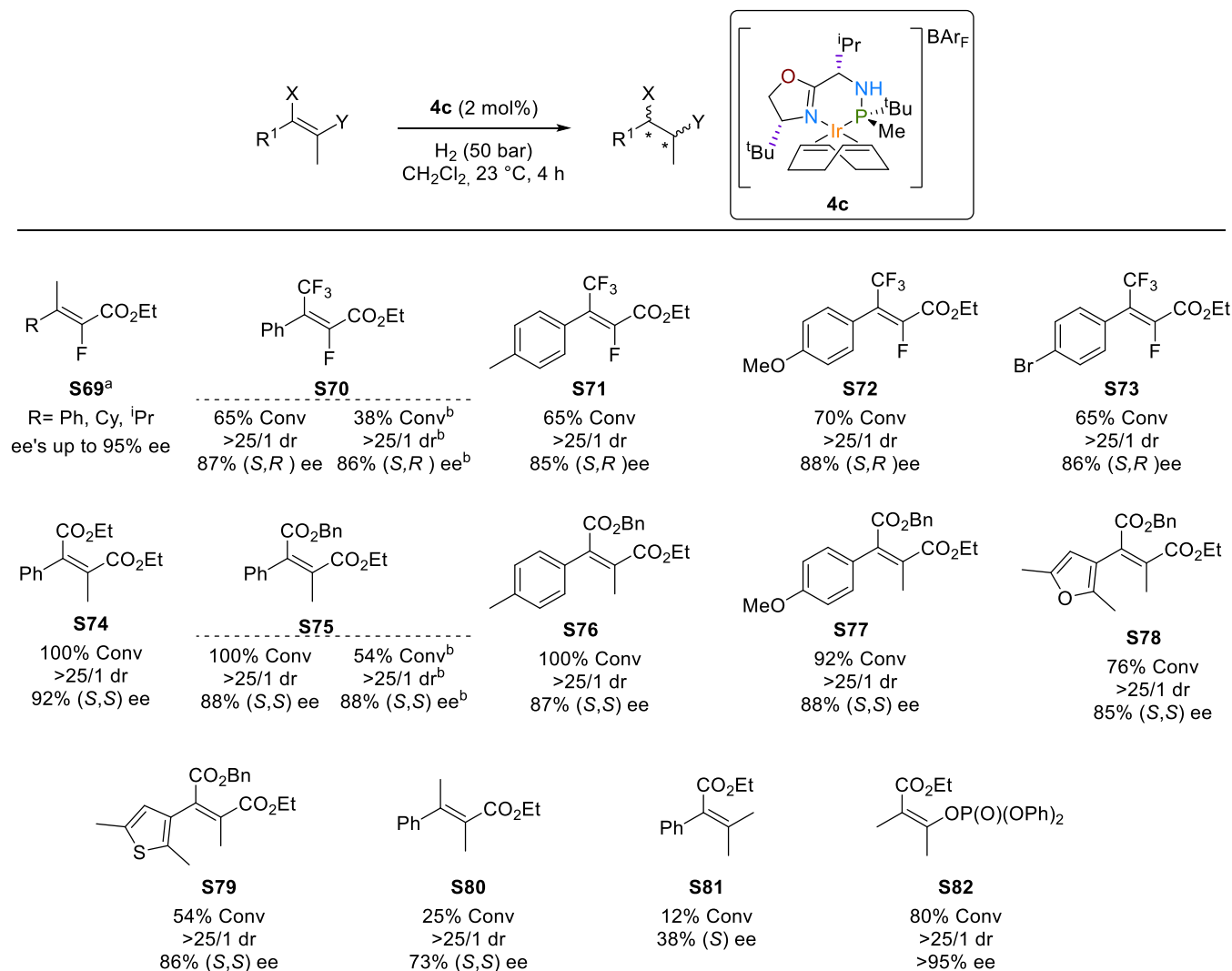
ester functionality such as substrates **S69** type (Scheme 6).^{8c} The challenge of these substrates is that the catalysts must not only control enantioselectivity but also diastereoselectivity (two vicinal stereogenic centers are created) and the defluorination side reaction. We first studied whether we could further expand the previous olefin scope to the reduction of the elusive vinyl fluoride **S70** with an ester functionality and also a CF_3 -functional group instead of the methyl group of **S69**.³² Improving on previous results reported in the literature (67% ee)^{10c} the reduction proceeded for the first time with high enantioselectivity (87% ee; Scheme 6), excellent diastereoselectivity without any defluorination with **4c**. The result is in line with the quadrant model developed for **4c** (vide supra, Figure 2a). The smallest substituent of the olefin (F) is placed in the most hindered quadrant (Q3) and the aryl substituent is in the semihindered quadrant Q1. According to this model, the predicted absolute configuration of the reduced product would be 2*S*, 3*R*, in agreement with the experimental result. Positively, the high enantioselectivity was extended for the first time to substrates with different aryl substituents **S71**–**S73** (Scheme 6).

Encouraged by these results, we then studied other functionalized tetrasubstituted olefins lacking a strong coordinative group. Due to the importance of succinic acid derivatives,³³ we focused on the asymmetric hydrogenation of tetrasubstituted maleates, with two vicinal ester groups (substrates **S74**–**S79**; Scheme 6), as an atom-efficient method for their preparation. The reactions with **4c** proceeded smoothly, providing the hydrogenated products with excellent diastereoselectivity (>25/1 dr) and high enantioselectivities (up to 92%). Moreover, the enantioselectivity was almost unaffected by the electronic nature of the aromatic group

(**S75**–**S77**) or the presence of heteroaromatic cyclic substituents (**S78** and **S79**).

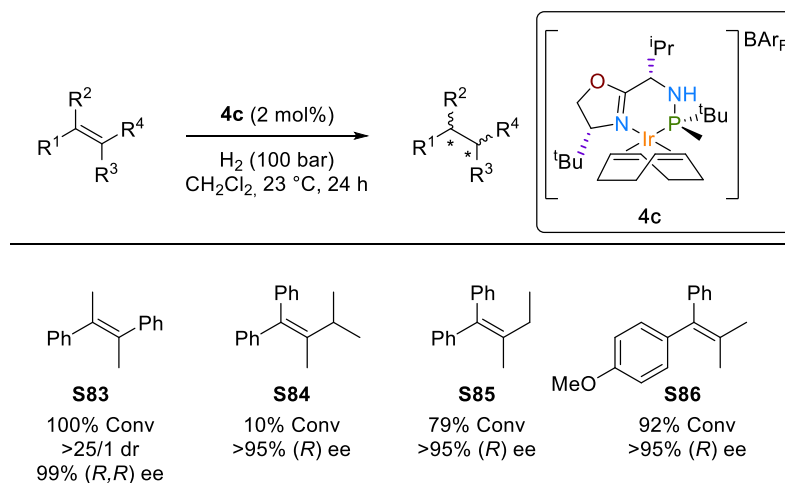
Next, we studied whether these results could be reproduced by replacing one of the ester groups with other substituents (Scheme 6). While the exchange of any of the esters by a methyl group (**S80** and **S81**) led to a decrease in activity and enantioselectivity (ee's up to 73%), positively the reduction of **S82**, with a phosphate instead of one of the ester groups, proceeded with high enantioselectivity (>95% ee) and diastereoselectivity (>25/1 dr), being the first time that this substrate class was hydrogenated.

Based on the recent findings by Gosselin and collaborators of an Ir–P,N catalyst applicable to a wide range of unfunctionalized tetrasubstituted acyclic olefins containing two or three aryl substituents,⁹ the scope of our iridium catalysts **1**–**4** was also studied in the reduction of some of these unfunctionalized olefins (Scheme 7 and the Supporting Information for pressure and catalyst loading effects). Initially, we studied the hydrogenation of substrate **S83**, having two phenyl groups in a *trans* disposition. In agreement with our quadrant model, high diastereo- and enantioselectivities were attained (>25/1 dr and 99% ee). Calculations performed for substrate **S83** with the catalyst **4c** reproduce the enantiomeric excess (computed 99% ee (*R,R*)) and support our quadrant model; see the Supporting Information for further details. We then proceed to study several *E*-1,2-dialkyl-1,2-diaryl olefins (**S84**–**S86**). Overcoming the limitations of Gosselin's system,⁹ our catalyst was able to differentiate the *Re*- and *Si*-faces in substrates differentiated only in the length of an alkyl substituent **S84** and **S85** and in the electronic properties of the aromatic substituents **S86**. Thus, enantioselectivities >95% ee were achieved for these elusive substrate types.

Scheme 6. Asymmetric Hydrogenation of Tetrasubstituted Olefins S69–S82^a

^aData from ref 8. ^bReaction carried out at 1 mol % of catalysts.

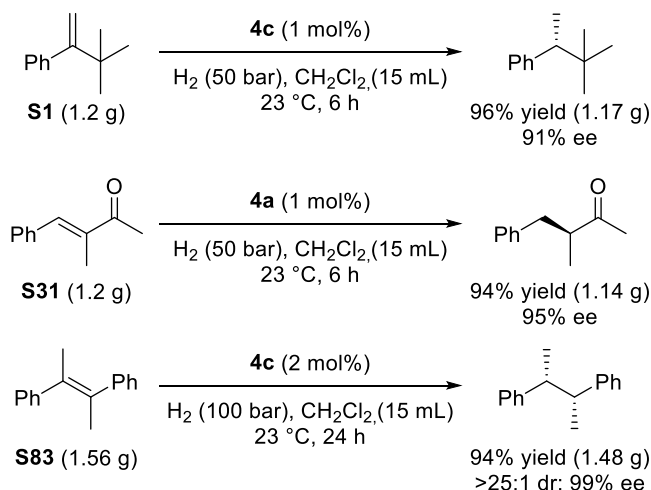
Scheme 7. Asymmetric Hydrogenation of Tetrasubstituted Olefins S83–S86



Finally, to show the potential utility of our catalysts, we also carried out the reaction of some representative di-, tri-, and

tetrasubstituted substrates (S1, S31, and S83) on a 7.5 mmol scale (Scheme 8).

Scheme 8. Practical Hydrogenation of S1, S31, and S83



CONCLUSIONS

In summary, we have shown that Ir-MaxPHOX catalysts (**1-4a-c**) that had been previously found to be successful in the asymmetric hydrogenation of nonfunctionalized cyclic and few acyclic-tetrasubstituted olefins are also good performers in the hydrogenation of a new set of 84 olefins which included di- and trisubstituted olefins, some with key poorly coordinative groups (such as lactams, lactones, enol phosphinates, ...) and some new examples of challenging tetrasubstituted alkenes. This family of Ir-MaxPHOX-type catalysts allowed the hydrogenation of exocyclic olefins, Z-olefins, pure alkyl-substituted olefins, and a broad range of tetrasubstituted olefins, thus improving over a previous family^{7b} also based on P,N ligands, that was so far the only one able to hydrogenate di-, tri-, and tetrasubstituted olefins. DFT calculations and deuterium labeling experiments allowed the rationalization of the stereochemical outcomes of the reactions and helped in the selection of suitable substrates for these Ir-MaxPHOX-type catalysts. The analysis of the TSs indicated that the high catalytic performance of these catalysts is due to their ability to adapt to the demands of each substrate. This ability also explains its excellent performance in the hydrogenation of functionalized olefins such as allyl amines and phthalimides,³⁴ cyclic α - and β -enamides,¹² and imines.³⁵ These results open a new perspective for the growth of ligand libraries for the asymmetric hydrogenation of nonchelating olefins, where the Ir/P-stereogenic aminophosphine-oxazoline catalysts could be a good choice for further development.

EXPERIMENTAL SECTION

General Considerations. All reactions were carried out using standard Schlenk techniques under an atmosphere of argon. Solvents were purified and dried by standard procedures. All reagents were used as received. Ir-catalyst precursors **1-4a-c** were prepared as previously reported.¹² ¹H and ¹³C{¹H} were recorded using a 400 MHz spectrometer. Chemical shifts are relative to that of SiMe₄ (¹H and ¹³C). ¹H and ¹³C assignments were made based on ¹H–¹H gCOSY and ¹H–¹³C gHSQC.

Typical Procedure for the Hydrogenation of Olefins.

The alkene (0.5 mmol) and Ir complex (1 or 2 mol %) were dissolved in CH₂Cl₂ (2 mL) in a high-pressure autoclave, which was purged four times with hydrogen. The apparatus

was pressurized to the desired pressure, and after the required reaction time, the autoclave was depressurized and the solvent evaporated. The residue was dissolved in Et₂O (1.5 mL) and filtered through a short Celite plug.

Computational Details. All species were optimized using the B3LYP¹⁵-D3¹⁶ functional as implemented in Gaussian 09.³⁶ The LANL2DZ³⁷ basis set together with the associated pseudopotential was used for iridium, and the 6-31G**³⁸ basis set was used for all other atoms. Implicit solvation using the PCM³⁹ model with the parameters for dichloromethane was included in geometry optimizations. The reported energies are Gibbs free energies in solution within the quasi-harmonic approximation to the Rigid Rotor Harmonic Oscillator Model proposed by Cramer and Truhlar;⁴⁰ corrections were done using the GoodVibes program.⁴¹ Single-point calculations were done using Grimme's standalone pure functional B97D3⁴² and the larger basis sets cc-pVTZ⁴³ for all atoms except for Ir, for which the cc-pVTZ-PP^{44,45} basis sets were used instead (see the Supporting Information).

Quadrant analysis was done by means of MolQuO (Quantitative Quadrant Diagram Representation of Molecular Systems).¹⁹ Note that this analysis was done taking the geometry of the whole TS, as shown in the figure, but removing the atoms of the olefin in the MolQuO calculation.

ASSOCIATED CONTENT

Supporting Information

The Supporting Information is available free of charge at <https://pubs.acs.org/doi/10.1021/acscatal.2c05579>.

Calculated energies and computed cartesian coordinates for all TSs; synthesis of substrates; characterization details and enantiomeric excess determination of hydrogenated products; copies of NMR spectra and GC or HPLC traces for ee determination of hydrogenated products, and hydrogenation experiments carried out in PC and deuteration experiments (PDF)

AUTHOR INFORMATION

Corresponding Authors

Xavier Verdager – *Institute for Research in Biomedicine (IRB Barcelona), The Barcelona Institute of Science and Technology (BIST), 08028 Barcelona, Spain; Departament de Química Inorgànica i Orgànica, Secció Química Orgànica, Universitat de Barcelona, 08028 Barcelona, Spain;*
 orcid.org/0000-0002-9229-969X;
 Email: xavier.verdager@irbbarcelona.org

Maria Besora – *Departament de Química Física i Inorgànica, Universitat Rovira i Virgili, 43007 Tarragona, Spain;*
 orcid.org/0000-0002-6656-5827; Email: maria.besora@urv.cat

Montserrat Diéguez – *Departament de Química Física i Inorgànica, Universitat Rovira i Virgili, 43007 Tarragona, Spain;*
 orcid.org/0000-0002-8450-0656;
 Email: montserrat.dieguez@urv.cat

Authors

Maria Biosca – *Departament de Química Física i Inorgànica, Universitat Rovira i Virgili, 43007 Tarragona, Spain;*
 orcid.org/0000-0002-9116-6318

Pol de la Cruz-Sánchez – Departament de Química Física i Inorgànica, Universitat Rovira i Virgili, 43007 Tarragona, Spain

Jorge Faiges – Departament de Química Física i Inorgànica, Universitat Rovira i Virgili, 43007 Tarragona, Spain

Jèssica Margalef – Departament de Química Física i Inorgànica, Universitat Rovira i Virgili, 43007 Tarragona, Spain

Ernest Salomó – Institute for Research in Biomedicine (IRB Barcelona), The Barcelona Institute of Science and Technology (BIST), 08028 Barcelona, Spain

Antoni Riera – Institute for Research in Biomedicine (IRB Barcelona), The Barcelona Institute of Science and Technology (BIST), 08028 Barcelona, Spain; Departament de Química Inorgànica i Orgànica, Secció Química Orgànica, Universitat de Barcelona, 08028 Barcelona, Spain;

orcid.org/0000-0001-7142-7675

Joan Ferré – Departament de Química Analítica i Química Orgànica, Universitat Rovira i Virgili, 43007 Tarragona, Spain

Feliu Maseras – Institute of Chemical Research of Catalonia (ICIQ), The Barcelona Institute of Science and Technology, 43007 Tarragona, Spain; orcid.org/0000-0001-8806-2019

Oscar Pàmies – Departament de Química Física i Inorgànica, Universitat Rovira i Virgili, 43007 Tarragona, Spain;

orcid.org/0000-0002-2352-8508

Complete contact information is available at:
<https://pubs.acs.org/10.1021/acscatal.2c05579>

Notes

The authors declare no competing financial interest.

ACKNOWLEDGMENTS

This work was supported by grants from the FEDER/Ministerio de Ciencia e Innovación (MICINN)/AEI (PID2019-104904GB-I00, PID2021-128128NB-I00, PID2020-115074GB-I00, PID2020-112825RB-I00, and CEX2019-000925-S). Grant 2017SGR1472, funded by the Catalan Government, is also gratefully acknowledged. ICIQ and IRB Barcelona are recipients of institutional funding from MICINN through the Centres of Excellence Severo Ochoa award and from the CERCA Program of the Catalan Government.

REFERENCES

- (1) (a) Noyori, R. *Asymmetric Catalysis in Organic Synthesis*; Wiley: New York, 1994. (b) *Comprehensive Asymmetric Catalysis*; Jacobsen, E. N.; Pfaltz, A.; Yamamoto, H., Eds.; Springer-Verlag: Berlin, 1999. (c) *Asymmetric Catalysis in Industrial Scale: Challenges, Approaches and Solutions*, 2nd ed.; Blaser, H.-U.; Federsel, H.-J., Eds.; Wiley: Weinheim, 2010. (d) *Catalytic Asymmetric Synthesis*, 4th ed.; Akiyama, T.; Ojima, I., Eds.; John Wiley & Sons, Inc: Hoboken, 2022.
- (2) (a) Busacca, C. A.; Fandrick, D. R.; Song, J. J.; Senanayake, C. H. The Growing Impact of Catalysis in the Pharmaceutical Industry. *Adv. Synth. Catal.* **2011**, *353*, 1825–1864. (b) Ager, D. J.; de Vries, A. H. M.; de Vries, J. G. Asymmetric homogeneous hydrogenations at scale. *Chem. Soc. Rev.* **2012**, *41*, 3340–3380. (c) Metal-Catalyzed Asymmetric Hydrogenation. Evolution and Prospect. In *Advance Catalysis*; Diéguez, M.; Pizzano, A., Eds.; Elsevier: Oxford, 2021; Vol. 68.
- (3) Biosca, M.; Diéguez, M.; Zanotti-Gerosa, A. Asymmetric Hydrogenation in Industry. In *Advances in Catalysis*; Elsevier, 2021; Vol. 68, pp 341–384.

- (4) See for example: (a) Genêt, J. P. *Modern Reduction Methods*; Andersson, P. G.; Munslow, I. J., Eds.; Wiley-VCH: Weinheim, 2008; pp 3–38. (b) Tang, W.; Zhang, X. New Chiral Phosphorus Ligands for Enantioselective Hydrogenation. *Chem. Rev.* **2003**, *103*, 3029–3069. (c) Chi, Y.; Tang, W.; Zhang, X. *Modern Rhodium-Catalyzed Organic Reactions*; Evans, P. A., Ed.; Wiley-VCH: Weinheim, 2005; pp 1–31. (d) Kitamura, M.; Noyori, R. *Ruthenium in Organic Synthesis*; Murahashi, S.-I., Ed.; Wiley-VCH: Weinheim, 2004; pp 3–52. (e) Weiner, B.; Szymanski, W.; Janssen, D. B.; Minnaard, A. J.; Feringa, B. L. Recent Advances in the Catalytic Asymmetric Synthesis of Beta-amino Acids. *Chem. Soc. Rev.* **2010**, *39*, 1656–1691. (f) Xie, J.-H.; Zhu, S.-F.; Zhou, Q.-L. Transition Metal-Catalyzed Enantioselective Hydrogenation of Enamines and Imines. *Chem. Rev.* **2011**, *111*, 1713–1760. (g) Etayo, P.; Vidal-Ferran, A. Rhodium-catalyzed asymmetric hydrogenation as a valuable synthetic tool for the preparation of chiral drugs. *Chem. Soc. Rev.* **2013**, *42*, 728–754. (h) Pizzano, A. Asymmetric Hydrogenation of Functionalized Olefins. In *Advances in Catalysis*; Elsevier, 2021; Vol. 68, pp 1–134. (i) Kim, A. N.; Stoltz, B. M. Recent advances in homogeneous catalysts for the asymmetric hydrogenation of heteroarenes. *ACS Catal.* **2020**, *10*, 13834–13851. (j) Cabré, A.; Verdager, X.; Riera, A. Recent advances in the enantioselective synthesis of chiral amines via transition metal-catalyzed asymmetric hydrogenation. *Chem. Rev.* **2022**, *122*, 269–339. (k) Zhang, Z.; Butt, N. A.; Zhang, W. Asymmetric Hydrogenation of Nonaromatic Cyclic Substrates. *Chem. Rev.* **2016**, *116*, 14769–14827.

- (5) (a) Cui, X.; Burgess, K. Catalytic Homogeneous Asymmetric Hydrogenations of Largely Unfunctionalized Alkenes. *Chem. Rev.* **2005**, *105*, 3272–3296. (b) Roseblade, S. J.; Pfaltz, A. Iridium-Catalyzed Asymmetric Hydrogenation of Olefins. *Acc. Chem. Res.* **2007**, *40*, 1402–1411. (c) Woodmansee, D. H.; Pfaltz, A. Asymmetric Hydrogenation of Alkenes Lacking Coordinating Groups. *Chem. Commun.* **2011**, *47*, 7912–7916. (d) Zhu, Y.; Burgess, K. Filling Gaps in Asymmetric Hydrogenation Methods for Acyclic Stereocontrol: Application to Chirons for Polyketide-Derived Natural Products. *Acc. Chem. Res.* **2012**, *45*, 1623–1636. (e) Verendel, J. J.; Pàmies, O.; Diéguez, M.; Andersson, P. G. Asymmetric Hydrogenation of Olefins Using Chiral Crabtree-type Catalysts: Scope and Limitations. *Chem. Rev.* **2014**, *114*, 2130–2169. (f) Margarita, C.; Andersson, P. G. Evolution and Prospects of the Asymmetric Hydrogenation of Unfunctionalized Olefins. *J. Am. Chem. Soc.* **2017**, *139*, 1346–1356. (g) Pàmies, O.; Zheng, J.; Faiges, J.; Andersson, P. G. Asymmetric Hydrogenation of Unfunctionalized Olefins or with Poorly Coordinative Groups. In *Advances in Catalysis*; Elsevier, 2021; Vol. 68, pp 135–203. For specific examples of application of P,O and P,S-ligands in the Ir-catalyzed asymmetric hydrogenation see: (h) Margalef, J.; Pàmies, O.; Pericas, M. A.; Diéguez, M. Evolution of phosphorus-thioether ligands for asymmetric catalysis. *Chem. Commun.* **2020**, *56*, 10795–10808. (i) Margalef, J.; Pericàs, M. A. Chiral Bidentate Heterodonor P-S/O Ligands. In *Chiral Ligands*; Diéguez, M., Ed.; CRC Press, 2021; pp 81–108. (j) Rageot, D.; Woodmansee, D. H.; Pugin, B.; Pfaltz, A. Proline-Based P,O Ligand/Iridium Complexes as Highly Selective Catalysts: Asymmetric Hydrogenation of Trisubstituted Alkenes. *Angew. Chem., Int. Ed.* **2011**, *50*, 9598–9601.

- (6) (a) Bell, S.; Wüstenberg, B.; Kaiser, S.; Menges, F.; Netscher, T.; Pfaltz, A. Asymmetric Hydrogenation of Unfunctionalized, Purely Alkyl-Substituted Olefins. *Science* **2006**, *311*, 642–644. (b) Wang, A.; Fraga, R. P. A.; Hörmann, E.; Pfaltz, A. Iridium-Catalyzed Asymmetric Hydrogenation of Unfunctionalized, Trialkyl-Substituted Olefins. *Chem. Asian J.* **2011**, *6*, 599–606.

- (7) The hydrogenation of such substrates is highly influenced by the size of substrate ring. So, for instance, a catalyst that provides high enantioselectivities in the hydrogenation of exocyclic olefins attached to a 5-membered ring motif is not suitable for the reduction of the 6-membered ring counterparts or vice versa. For non-functionalized olefins, see for instance: (a) Xia, J.; Yang, G.; Zhuge, R.; Liu, Y.; Zhang, W. Iridium-Catalyzed Asymmetric Hydrogenation of Unfunctionalized Exocyclic C=C Bonds. *Chem. - Eur. J.* **2016**, *22*, 18354–18357. (up to 97% for benzofused 5-membered ring olefins

- and 75% ee for 6-membered ring counterparts) (b) Biosca, M.; Magre, M.; Pàmies, O.; Diéguez, M. Asymmetric Hydrogenation of Disubstituted, Trisubstituted, and Tetrasubstituted Minimally Functionalized Olefins and Cyclic β -Enamides with Easily Accessible Ir-P,Oxazoline Catalysts. *ACS Catal.* **2018**, *8*, 10316–10320. (up to 93% for benzofused 5-membered ring olefins and 30% ee for 6-membered ring counterparts) (c) Biosca, M.; de la Cruz-Sánchez, P.; Tarr, D.; Llanes, P.; Karlsson, E. A.; Margalef, J.; Pàmies, O.; Pericàs, M. A.; Diéguez, M. Filling the gaps in the challenging asymmetric hydrogenation of exocyclic benzofused-based alkenes with Ir-P,N catalysts. *Adv. Synth. Catal.* **2023**, *365*, 167–177. (up to 96% and 99% for benzofused 5- and 6-membered ring olefins, respectively, and 40% ee for the 4-membered ring counterpart). For olefins with poorly coordinative groups, see for instance: (d) Tian, F.; Yao, D.; Liu, Y.; Xie, F.; Zhang, W. Iridium-Catalyzed Highly Enantioselective Hydrogenation of Exocyclic α,β -Unsaturated Carbonyl Compounds. *Adv. Synth. Catal.* **2010**, *352*, 1841–1845. (up to 99% ee for 5-membered ring cyclic enones, lactones and lactams and up to 75% ee for 6-membered ring counterparts) (e) Liu, X.; Han, Z.; Wang, Z.; Ding, K. SpinPhox/Iridium(I)-Catalyzed Asymmetric Hydrogenation of Cyclic α -Alkylidene Carbonyl Compounds. *Angew. Chem., Int. Ed.* **2014**, *53*, 1978–1982. (up to 98% ee for 6-membered ring cyclic enones, lactones and lactams and up to 83% ee for 5-membered ring counterparts) (f) Xia, J.; Nie, Y.; Yang, G.; Liu, Y.; Gridnev, I. D.; Zhang, W. Ir-Catalyzed Asymmetric Hydrogenation of α -Alkylidene β -Lactams and Cyclobutanones. *Chin. J. Chem.* **2018**, *36*, 612–618. (catalysts specially designed for 4-membered ring cyclic enones and lactams; ee's up to 98%) (g) Margalef, J.; Biosca, M.; de la Cruz-Sánchez, P.; Caldentey, X.; Rodríguez-Esrich, C.; Pàmies, O.; Pericàs, M. A.; Diéguez, M. Indene Derived Phosphorus-Thioether Ligands for the Ir-Catalyzed Asymmetric Hydrogenation of Olefins with Diverse Substitution Patterns and Different Functional Groups. *Adv. Synth. Catal.* **2021**, *363*, 4561–4574. (catalysts designed for 6-membered ring cyclic enones, lactones and lactams; ee's up to 99%)
- (8) (a) Schrems, M. G.; Neumann, E.; Pfaltz, A. Iridium-Catalyzed Asymmetric Hydrogenation of Unfunctionalized Tetrasubstituted Olefins. *Angew. Chem., Int. Ed.* **2007**, *46*, 8274–8276. (b) Busacca, C. A.; Qu, B.; Grêt, N.; Fandrick, K. R.; Saha, A. K.; Marsini, M.; Reeves, D.; Haddad, N.; Eriksson, M.; Wu, J. P.; Grinberg, N.; Lee, H.; Li, Z.; Lu, B.; Chen, D.; Hong, Y.; Ma, S.; Senanayake, C. H. Tuning the Peri Effect for Enantioselectivity: Asymmetric Hydrogenation of Unfunctionalized Olefins with the BIPI Ligands. *Adv. Synth. Catal.* **2013**, *355*, 1455–1463. (c) Biosca, M.; Salomó, E.; de la Cruz-Sánchez, P.; Riera, A.; Verdaguer, X.; Pàmies, O.; Diéguez, M. Extending the Substrate Scope in the Hydrogenation of Unfunctionalized Tetrasubstituted Olefins with Ir-P Stereogenic Aminophosphine–Oxazoline Catalysts. *Org. Lett.* **2019**, *21*, 807–811.
- (9) Bigler, R.; Mack, K. A.; Shen, J.; Tosatti, P.; Han, C.; Bachmann, S.; Zhang, H.; Scalone, M.; Pfaltz, A.; Denmark, S. E.; Hildbrand, S.; Gosselin, F. Asymmetric Hydrogenation of Unfunctionalized Tetrasubstituted Acyclic Olefins. *Angew. Chem., Int. Ed.* **2020**, *59*, 2844–2849.
- (10) (a) Kerdphon, S.; Ponra, S.; Yang, J.; Wu, H.; Eriksson, L.; Andersson, P. G. Diastereo- and Enantioselective Synthesis of Structurally Diverse Succinate, Butyrolactone, and Trifluoromethyl Derivatives by Iridium-Catalyzed Hydrogenation of Tetrasubstituted Olefins. *ACS Catal.* **2019**, *9*, 6169–6176. (b) Zhao, Q.-K.; Wu, X.; Li, L.-P.; Yang, F.; Xie, J.-H.; Zhou, Q.-L. Asymmetric Hydrogenation of β -Aryl Alkylidene Malonate Esters: Installing an Ester Group Significantly Increases the Efficiency. *Org. Lett.* **2021**, *23*, 1675–1680. (c) Ponra, S.; Rabten, W.; Yang, J.; Wu, H.; Kerdphon, S.; Andersson, P. G. Diastereo- and enantioselective synthesis of fluorine motifs with two contiguous stereogenic centers. *J. Am. Chem. Soc.* **2018**, *140*, 13878–13883.
- (11) (a) Pfaltz, A.; Drury, W. J., III Design of chiral ligands for asymmetric catalysis: From C₂-symmetric P,P- and N,N-ligands to sterically and electronically nonsymmetrical P,N-ligands. *Proc. Natl. Acad. Sci. U.S.A.* **2004**, *101*, 5723–5726. (b) Yoon, T. P.; Jacobsen, E. N. Privileged chiral catalysts. *Science* **2003**, *299*, 1691–1693.
- (c) Sommer, W.; Weibel, D. Asymmetric Catalysis, Privileged Ligands and Complexes. *Sigma Aldrich's ChemFiles* **2008**, *2*, 1–91.
- (d) *Privileged Chiral Ligands and Catalysts*; Zhou, Q., Ed.; John Wiley & Sons Inc.: New York, 2011. (e) *Chiral Ligands. Evolution of Ligand Libraries for Asymmetric Catalysis*; Diéguez, M., Ed.; CRC Press: Boca Raton, 2021.
- (12) (a) Salomó, E.; Orgué, S.; Riera, A.; Verdaguer, X. Highly Enantioselective Iridium-Catalyzed Hydrogenation of Cyclic Enamides. *Angew. Chem., Int. Ed.* **2016**, *55*, 7988–7992. The Ir-MaxPHOX library has also been applied in the asymmetric hydrogenation of functionalized olefins and imines as well as in the isomerization of alkenes, see: (b) Cabré, A.; Riera, T.; Verdaguer, X. P-Stereogenic Amino-Phosphines as Chiral Ligands: From Privileged Intermediates to Asymmetric Catalysis. *Acc. Chem. Res.* **2020**, *53*, 676–689.
- (13) To the best of our knowledge so far only one family of Ir-catalysts has been successfully applied to di-, tri- and tetrasubstituted olefins, see ref 7b.
- (14) (a) Bayardon, J.; Holz, J.; Schäffner, B.; Andrushko, V.; Verevkin, S. P.; Preetz, A.; Börner, A. Propylene Carbonate as a Solvent for Asymmetric Hydrogenations. *Angew. Chem., Int. Ed.* **2007**, *46*, 5971–5974. (b) Schäffner, B.; Holz, J.; Verevkin, S. P.; Börner, A. Organic carbonates as alternative solvents for palladium-catalyzed substitution reactions. *ChemSusChem* **2008**, *1*, 249–253. (c) Schäffner, B.; Schäffner, B.; Verevkin, S. P.; Börner, A. Organic carbonates as solvents in synthesis and catalysis. *Chem. Rev.* **2010**, *110*, 4554–4581.
- (15) (a) Becke, A. D. Density-functional thermochemistry. III. The role of exact exchange. *J. Chem. Phys.* **1993**, *98*, 5648–5652. (b) Stephens, P. J.; Devlin, F. J.; Chabalowski, C. F.; Frisch, M. J. Ab Initio Calculation of Vibrational Absorption and Circular Dichroism Spectra Using Density Functional Force Fields. *J. Phys. Chem. A* **1994**, *98*, 11623–11627.
- (16) Grimme, S.; Antony, J.; Ehrlich, S.; Krieg, H. A consistent and accurate ab initio parametrization of density functional dispersion correction (DFT-D) for the 94 elements H-Pu. *J. Chem. Phys.* **2010**, *132*, No. 154104.
- (17) (a) Brandt, P.; Hedberg, C.; Andersson, P. G. New Mechanistic Insights into the Iridium-Phosphanooxazoline-Catalyzed Hydrogenation of Unfunctionalized Olefins: A DFT and Kinetic Study. *Chem. - Eur. J.* **2003**, *9*, 339–347. (b) Fan, Y.; Cui, X.; Burgess, K.; Hall, M. B. Electronic effects steer the mechanism of asymmetric hydrogenations of unfunctionalized aryl-substituted alkenes. *J. Am. Chem. Soc.* **2004**, *126*, 16688–16689. (c) Cui, X.; Fan, Y.; Hall, M. B.; Burgess, K. Mechanistic Insights into Iridium-Catalyzed Asymmetric Hydrogenation of Dienes. *Chem. - Eur. J.* **2005**, *11*, 6859–6868. (d) Church, T. L.; Rasmussen, T.; Andersson, P. G. Enantioselectivity in the Iridium-Catalyzed Hydrogenation of Unfunctionalized Olefins. *Organometallics* **2010**, *29*, 6769–6781. (e) Hopmann, K. H.; Bayer, A. On the mechanism of iridium-catalyzed asymmetric hydrogenation of imines and alkenes: A theoretical study. *Organometallics* **2011**, *30*, 2483–2497. (f) Mazuela, J.; Norrby, P.-O.; Andersson, P. G.; Pàmies, O.; Diéguez, M. Pyranoside Phosphite–Oxazoline Ligands for the Highly Versatile and Enantioselective Ir-Catalyzed Hydrogenation of Minimally Functionalized Olefins. A Combined Theoretical and Experimental Study. *J. Am. Chem. Soc.* **2011**, *133*, 13634–13645. (g) Gruber, S.; Pfaltz, A. Asymmetric hydrogenation with iridium C, N and N, P ligand complexes: characterization of dihydride intermediates with a coordinated alkene. *Angew. Chem., Int. Ed.* **2014**, *53*, 1896–1900.
- (18) Alvarez-Moreno, M.; de Graaf, C.; Lopez, N.; Maseras, F.; Poblet, J. M.; Bo, C. Managing the Computational Chemistry Big Data Problem: The ioChem-BD Platform. *J. Chem. Inf. Model.* **2015**, *55*, 95–103.
- (19) (a) Aguado-Ullate, S.; Saureu, S.; Guasch, L.; Carbo, J. J. Theoretical Studies of Asymmetric Hydroformylation Using the Rh-(R,S)-BINAPHOS Catalyst – Origin of Coordination Preferences and Stereoinduction. *Chem. - Eur. J.* **2012**, *18*, 995–1005. (b) Aguado-Ullate, S.; Urbano-Cuadrado, M.; Villalba, I.; Pires, E.; Garcia, J. I.; Bo, C.; Carbó, J. J. Predicting the Enantioselectivity of the Copper-Catalyzed Cyclopropanation of Alkenes by Using Quantitative

Quadrant-Diagram Representations of the Catalysts. *Chem. - Eur. J.* **2012**, *18*, 14026–14036.

(20) Note, that this analysis was performed by taking the geometry of the whole TS, as shown in the figure, but removing the olefin atoms in the MolQuO calculation.

(21) (a) Mazuela, J.; Verendel, J. J.; Coll, M.; Schäffner, B.; Börner, A.; Andersson, P. G.; Pàmies, O.; Diéguez, M. Iridium Phosphite-Oxazoline Catalysts for the Highly Enantioselective Hydrogenation of Terminal Alkenes. *J. Am. Chem. Soc.* **2009**, *131*, 12344–12353. (b) Pàmies, O.; Andersson, P. G.; Diéguez, M. Asymmetric Hydrogenation of Minimally Functionalised Terminal Olefins: An Alternative Sustainable and Direct Strategy for Preparing Enantioenriched Hydrocarbons. *Chem. - Eur. J.* **2010**, *16*, 14232–14240.

(22) (a) Blankenstein, J.; Pfaltz, A. A New Class of Modular Phosphinite–Oxazoline Ligands: Ir-Catalyzed Enantioselective Hydrogenation of Alkenes. *Angew. Chem., Int. Ed.* **2001**, *40*, 4445–4447. (b) McIntyre, S.; Hörmann, E.; Menges, F.; Smidt, S. P.; Pfaltz, A. Iridium-Catalyzed Enantioselective Hydrogenation of Terminal Alkenes. *Adv. Synth. Catal.* **2005**, *347*, 282–288. (c) Biosca, M.; Paptchikhine, A.; Pàmies, O.; Andersson, P. G.; Diéguez, M. Extending the Substrate Scope of Bicyclic P-Oxazoline/Thiazole Ligands for Ir-Catalyzed Hydrogenation of Unfunctionalized Olefins by Introducing a Biaryl Phosphoroamidite Group. *Chem. - Eur. J.* **2015**, *21*, 3455–3464. (d) Krajangri, S.; Wu, H.; Liu, J.; Rabten, W.; Singhand, T.; Andersson, P. G. Tandem Peterson olefination and chemoselective asymmetric hydrogenation of β -hydroxy silanes. *Chem. Sci.* **2019**, *10*, 3649–3653.

(23) (a) Fessard, T. C.; Andrews, S. P.; Motoyohsi, H.; Carreira, E. Enantioselective Preparation of 1, 1-Diarylethanes: Aldehydes as Removable Steering Groups for Asymmetric Synthesis. *Angew. Chem., Int. Ed.* **2007**, *46*, 9331–9334. (b) Prat, L.; Dupas, G.; Duflos, J.; Quéguiner, G.; Bourguignon, J.; Levacher, V. Deracemization of alkyl diarylmethanes using (–)-sparteine or a chiral proton source. *Tetrahedron Lett.* **2001**, *42*, 4515–4518. (c) Wilkinson, J. A.; Rossington, S. B.; Ducki, S.; Leonard, J.; Hussain, N. Asymmetric alkylation of diarylmethane derivatives. *Tetrahedron* **2006**, *62*, 1833–1844.

(24) Pure alkyls are difficult to study because the enantiomers of pure hydrocarbons are difficult to separate. This was also the case of the substrate (E)-3,4,4-trimethylpent-2-ene (with a tBu group), whose measurement of ee failed despite we obtained 100% conversion.

(25) (a) Donde, Y.; Nguyen, J. H. WO2015048553A12015. (b) Pohlski, F.; Lange, U.; Ochse, M.; Behi, B.; Hutchins, C. W. US2012040948A12012. (c) Lansbury, P. T.; Justman, C. J. WO2009036275A12009. (d) Pontillo, J.; Gao, Y.; Wade, W. S.; Wu, D.; Eccles, W. K. U.S. Patent US2006276454A12006. (e) Kolanos, R.; Siripurapu, U.; Pullagurra, M.; Riaz, M.; Setola, V.; Roth, B. L.; Dukat, M.; Glennon, R. A. Binding of isotryptamines and indenes at h5-HT6 serotonin receptors. *Bioorg. Med. Chem. Lett.* **2005**, *15*, 1987–1991. (f) Horwell, D. C.; Howson, W.; Nolan, W. P.; Ratcliffe, G. S.; Rees, D. C.; Willems, H. M. G. The design of dipeptide helical mimetics, Part I: the synthesis of 1,6-disubstituted indanes. *Tetrahedron* **1995**, *51*, 203–211. (g) Plummer, E. L.; Tonawanda, N. U.S. Patent US4136274A11982. (h) Ardalani, H.; Avan, A.; Ghayour-Mobarhan, M. Podophyllotoxin: a novel potential natural anticancer agent. *Avicenna J. Phytomed.* **2017**, *7*, 285–294. (i) Cervo, L.; Samanin, R. Potential antidepressant properties of 8-hydroxy-2-(di-n-propylamino) tetralin, a selective serotonin IA receptor agonist. *Eur. J. Pharm.* **1987**, *144*, 223–229.

(26) Biosca, M.; Magre, M.; Coll, M.; Pàmies, O.; Diéguez, M. Alternatives to Phosphinooxazoline (t-BuPHOX) Ligands in the Metal-Catalyzed Hydrogenation of Minimally Functionalized Olefins and Cyclic β -Enamides. *Adv. Synth. Catal.* **2017**, *359*, 2801–2814.

(27) Much recently it has been disclosed that the high enantiocontrol for these substrates can be further expanded to both 5- and 6-membered ring counterparts by introducing a triazole in the ligand design, see ref. 7c.

(28) (a) Rageot, D.; Woodmansee, D. H.; Pugin, B.; Pfaltz, A. Proline- Based P,O Ligand/Iridium Complexes as Highly Selective

Catalysts: Asymmetric Hydrogenation of Trisubstituted Alkenes. *Angew. Chem., Int. Ed.* **2011**, *50*, 9598–9601. (b) Xi, J. Q.; Quan, X.; Andersson, P. G. Highly Enantioselective Iridium-Catalyzed Hydrogenation of α,β -Unsaturated Esters. *Chem. - Eur. J.* **2012**, *18*, 10609–10616. (c) Woodmansee, D. H.; Müller, M. A.; Tröndlin, L.; Hörmann, E.; Pfaltz, A. Asymmetric Hydrogenation of α,β -Unsaturated Carboxylic Esters with Chiral Iridium N, P Ligand Complexes. *Chem. - Eur. J.* **2012**, *18*, 13780–13786. (d) Lu, S. M.; Bolm, C. Highly Enantioselective Synthesis of Optically Active Ketones by Iridium-Catalyzed Asymmetric Hydrogenation. *Angew. Chem., Int. Ed.* **2008**, *47*, 8920–8923. (e) Lu, W.-J.; Chen, Y.-W.; Hou, X.-L. Iridium-Catalyzed Highly Enantioselective Hydrogenation of the C–C Bond of α,β -Unsaturated Ketones. *Angew. Chem., Int. Ed.* **2008**, *47*, 10133–10136. (f) Shang, J.; Han, Z.; Li, Y.; Wang, Z.; Ding, K. Highly enantioselective asymmetric hydrogenation of (E)- β,β -disubstituted α,β -unsaturated Weinreb amides catalyzed by Ir (I) complexes of SpinPhox ligands. *Chem. Commun.* **2012**, *48*, 5172–5174. (g) Biosca, M.; Pàmies, O.; Diéguez, M. Giving a Second Chance to Ir/ Sulfoximine-Based Catalysts for the Asymmetric Hydrogenation of Olefins Containing Poorly Coordinative Groups. *J. Org. Chem.* **2019**, *84*, 8259–8266.

(29) Chiral organofluorines are important in agrochemicals and drug synthesis among other applications due to its unique physical properties. For a recent hydrogenation of this substrate class, see: Ponra, S.; Yang, J.; Kerdphon, S.; Andersson, P. G. Asymmetric Synthesis of Alkyl Fluorides: Hydrogenation of Fluorinated Olefins. *Angew. Chem., Int. Ed.* **2019**, *58*, 9282–9287.

(30) (a) Cheruku, P.; Gohil, S.; Andersson, P. G. Asymmetric hydrogenation of enol phosphinates by iridium catalysts having N,P ligands. *Org. Lett.* **2007**, *9*, 1659–1661. (b) Cheruku, P.; Diesen, J.; Andersson, P. G. Asymmetric Hydrogenation of Di and Trisubstituted Enol Phosphinates with N,P- Ligated Iridium Complexes. *J. Am. Chem. Soc.* **2008**, *130*, 5595–5599. (c) Paptchikhine, A.; Cheruku, P.; Engman, M.; Andersson, P. G. Iridium-catalyzed enantioselective hydrogenation of vinyl boronates. *Chem. Commun.* **2009**, 5996–5998. (d) Ganic, A.; Pfaltz, A. Iridium-Catalyzed Enantioselective Hydrogenation of Alkenylboronic Esters. *Chem. - Eur. J.* **2012**, *18*, 6724–6728.

(31) See for instance: (a) Theodore, L. J.; Nelson, W. L. Stereospecific synthesis of the enantiomers of verapamil and gallopamil. *J. Org. Chem.* **1987**, *52*, 1309–1315. (b) Procopiou, P. A.; Biggadike, K.; English, A. F.; Farrell, R. M.; Hagger, G. N.; Hancock, A. P.; Haase, M. V.; Irving, W. R.; Snowden, M. A.; Solanke, Y. E.; Tralau-Stewart, C. J.; Walton, S. E.; Wood, J. A. Novel Glucocorticoid Antedrug Possessing a 17 β -(γ -Lactone) Ring. *J. Med. Chem.* **2001**, *44*, 602–612. (c) Adlington, R. M.; Baldwin, J. E.; Becker, G. W.; Chen, B.; Cheng, L.; Cooper, S. L.; Hermann, R. B.; Howe, T. J.; McCoull, W.; McNulty, A. M.; Neubauer, B. L.; Pritchard, G. J. Design, synthesis, and proposed active site binding analysis of monocyclic 2-azetidione inhibitors of prostate specific antigen. *J. Med. Chem.* **2001**, *44*, 1491–1508. (d) Aoyama, Y.; Uenaka, M.; Kii, M.; Tanaka, M.; Konoike, T.; Hayasaki-Kajiwara, Y.; Naya, N.; Nakajima, M. Design, synthesis and pharmacological evaluation of 3-benzylazetidione-2-one-based human chymase inhibitors. *Bioorg. Med. Chem.* **2001**, *9*, 3065–3075. (e) Kottirsch, G.; Koch, G.; Feifel, R.; Neumann, U. β -Aryl-Succinic Acid Hydroxamates as Dual Inhibitors of Matrix Metalloproteinases and Tumor Necrosis Factor Alpha Converting Enzyme. *J. Med. Chem.* **2002**, *45*, 2289–2293. (f) Higashi, T.; Isobe, Y.; Ouchi, H.; Suzuki, H.; Okazaki, Y.; Asakawa, T.; Furuta, T.; Wakimoto, T.; Kan, T. Stereocontrolled Synthesis of (+)-Methoxyphenylkainic Acid and (+)-Phenylkainic Acid. *Org. Lett.* **2011**, *13*, 1089–1091. (g) Shan, W.; Balog, A.; Quesnelle, C.; Gill, P.; Han, W.-C.; Norris, D.; Mandal, S.; Thiruvankadam, R.; Gona, K. B.; Thiyagarajan, K.; Kandeula, S.; McGlinchey, K.; Menard, K.; Wen, M.-L.; Rose, A.; White, R.; Guarino, V.; Shen, D. R.; Cvijic, M. E.; Ransinghe, A.; Dai, J.; Zhang, Y.; Wu, D.-R.; Mathur, A.; Rampulla, R.; Trainor, G.; Hunt, J. T.; Vite, G. D.; Westhouse, R.; Lee, F. Y.; Gavai, A. V. BMS-871: A novel orally active pan-Notch inhibitor as an anticancer agent. *Bioorg. Med.*

- Chem. Lett.* **2015**, *25*, 1905–1909. (h) Lin, X.; Yuen, P.-W.; Mendonca, R.; Parr, B.; Pastor, R.; Pei, Z.; Gaz-zard, L.; Jaipuri, F.; Kumar, S.; Li, X.; Pavana, R.; Potturi, H.; Velvadapu, V.; Waldo, J.; Zhang, Z.; Wu, G. WO2017107979A12017. (i) Kaieda, A.; Toyofuku, M.; Daini, M.; Nara, H.; Yoshikawa, M.; Ishii, N.; Hidaka, K. U.S. Patent. US20170015655A12017. (j) Huang, X.; Brubaker, J.; Peterson, S. L.; Butcher, J. W.; Close, J. T.; Martinez, M.; Maccoss, R. N.; Jung, J. O.; Siliphaivanh, P.; Zhang, H.; Aslanian, R. G.; Biju, P. J.; Dong, L.; Huang, Y.; McCormick, K. D.; Palani, A.; Shao, N.; Zhou, W. WO2012174176A12017.
- (32) Chiral CF₃-containing molecules are of interest because the trifluoromethyl motif often occurs in pharmaceuticals and agrochemical products, see for instance (a) Jeschke, P. The Unique Role of Fluorine in the Design of Active Ingredients for Modern Crop Protection. *ChemBioChem* **2004**, *5*, 570–589. (b) Zhou, Y.; Wang, J.; Gu, Z.; Wang, S.; Zhu, W.; Aceña, J. L.; Soloshonok, V. A.; Izawa, K.; Liu, H. Next Generation of Fluorine-Containing Pharmaceuticals, Compounds Currently in Phase II–III Clinical Trials of Major Pharmaceutical Companies: New Structural Trends and Therapeutic Areas. *Chem. Rev.* **2016**, *116*, 422–518. (c) Yang, J.; Ponra, S.; Li, X.; Peters, B. B. C.; Massaro, L.; Zhou, T.; Andersson, P. G. Catalytic enantioselective synthesis of fluoromethylated stereocenters by asymmetric hydrogenation. *Chem. Sci.* **2022**, *13*, 8590–8596.
- (33) See for example (a) Kammermeier, B.; Beck, G.; Holla, W.; Jacobi, D.; Napierski, B.; Jendralla, H. Vanadium(II)- and Niobium(III)-Induced, Diastereoselective Pinacol Coupling of Peptide Aldehydes to Give a C₂-Symmetrical HIV Protease Inhibitor. *Chem. - Eur. J.* **1996**, *2*, 307–315. (b) Fabre, B.; Ramos, A.; Pascual-Teresa, B. Targeting Matrix Metalloproteinases: Exploring the Dynamics of the S1' Pocket in the Design of Selective, Small Molecule Inhibitors. *J. Med. Chem.* **2014**, *57*, 10205–10219. (c) Vandenbroucke, R. E.; Libert, C. Is there new hope for therapeutic matrix metalloproteinase inhibition? *Nat. Rev. Drug Discovery* **2014**, *13*, 904–927. (d) Stuart, A.; McCallum, M. M.; Fan, D.; LeCaptain, D. J.; Lee, C. Y.; Mohanty, D. K. Poly(vinyl chloride) plasticized with succinate esters: synthesis and characterization. *Polym. Bull.* **2010**, *65*, 589–598.
- (34) (a) Cabré, A.; Romagnoli, E.; Martínez-Balart, P.; Verdager, X.; Riera, A. Highly Enantioselective Iridium-Catalyzed Hydrogenation of 2-Aryl Allyl Phthalimides. *Org. Lett.* **2019**, *21*, 9709–9713. (b) Rojo, P.; Molinari, M.; Cabré, A.; García-Mateos, C.; Riera, A.; Verdager, X. Iridium-Catalyzed Asymmetric Hydrogenation of 2,3-Diaryllallyl Amines with a Threonine-Derived P-Stereogenic Ligand for the Synthesis of Tetrahydroquinolines and Tetrahydroisoquinolines. *Angew. Chem., Int. Ed.* **2022**, *61*, No. e202204300.
- (35) (a) Salomó, E.; Rojo, P.; Hernández-Lladó, P.; Riera, A.; Verdager, X. P-Stereogenic and Non-P-Stereogenic Ir-MaxPHOX in the Asymmetric Hydrogenation of N-Aryl Imines. Isolation and X-Ray Analysis of Imine Iridacycles. *J. Org. Chem.* **2018**, *83*, 4618–4627. (b) Salomó, E.; Gallen, A.; Sciortino, G.; Ujaque, G.; Grabulosa, A.; Lledós, A.; Riera, A.; Verdager, X. Direct Asymmetric Hydrogenation of N-Methyl and N-Alkyl Imines with an Ir(III)H Catalyst. *J. Am. Chem. Soc.* **2018**, *140*, 16967–16970.
- (36) Frisch, M. J.; Trucks, G. W.; Schlegel, H. B.; Scuseria, G. E.; Robb, M. A.; Cheeseman, J. R.; Scalmani, G.; Barone, V.; Petersson, G. A.; Nakatsuji, H.; Li, X.; Caricato, M.; Marenich, A.; Bloino, J.; Janesko, B. G.; Gomperts, R.; Mennucci, B.; Hratchian, H. P.; Ortiz, J. V.; Izmaylov, A. F.; Sonnenberg, J. L.; Williams-Young, D.; Ding, F.; Lipparini, F.; Egidi, F.; Goings, J.; Peng, B.; Petrone, A.; Henderson, T.; Ranasinghe, D.; Zakrzewski, V. G.; Gao, J.; Rega, N.; Zheng, G.; Liang, W.; Hada, M.; Ehara, M.; Toyota, K.; Fukuda, R.; Hasegawa, J.; Ishida, M.; Nakajima, T.; Honda, Y.; Kitao, O.; Nakai, H.; Vreven, T.; Throssell, K.; Montgomery, J. A., Jr; Peralta, J. E.; Ogliaro, F.; Bearpark, M.; Heyd, J. J.; Brothers, E.; Kudin, K. N.; Staroverov, V. N.; Keith, T.; Kobayashi, R.; Normand, J.; Raghavachari, K.; Rendell, A.; Burant, J. C.; Iyengar, S. S.; Tomasi, J.; Cossi, M.; Millam, J. M.; Klene, M.; Adamo, C.; Cammi, R.; Ochterski, J. W.; Martin, R. L.; Morokuma, K.; Farkas, O.; Foresman, J. B.; Fox, D. J. *Gaussian 09*, Revision A.02; Gaussian, Inc., 2016.
- (37) (a) Hay, P. J.; Wadt, W. R. Ab initio effective core potentials for molecular calculations. Potentials for the transition metal atoms Sc to Hg. *J. Chem. Phys.* **1985**, *82*, 270–283. (b) Hay, P. J.; Wadt, W. R. Ab initio effective core potentials for molecular calculations. Potentials for K to Au including the outermost core orbitals. *J. Chem. Phys.* **1985**, *82*, 299–310.
- (38) Petersson, G. A.; Bennett, A.; Tensfeldt, T. G.; Al-Laham, M. A.; Shirley, W. A.; Mantzaris, J. A complete basis set model chemistry. I. The total energies of closed-shell atoms and hydrides of the first-row atoms. *J. Chem. Phys.* **1988**, *89*, 2193–2218.
- (39) Tomasi, J.; Mennucci, B.; Cammi, R. Quantum Mechanical Continuum Solvation Models. *Chem. Rev.* **2005**, *105*, 2999–3094.
- (40) Ribeiro, R. F.; Marenich, A. V.; Cramer, C. J.; Truhlar, D. G. Use of Solution-Phase Vibrational Frequencies in Continuum Models for the Free Energy of Solvation. *J. Phys. Chem. B* **2011**, *115*, 14556–14562.
- (41) Luchini, G.; Alegre-Requena, J. V.; Funes-Ardoiz, I.; Paton, R. S. GoodVibes: Automated Thermochemistry for Heterogeneous Computational Chemistry Data. *F1000Research* **2020**, *9*, No. 291.
- (42) (a) Grimme, S. Semiempirical GGA-type density functional constructed with a long-range dispersion correction. *J. Comput. Chem.* **2006**, *27*, 1787–1799. (b) Grimme, S.; Ehrlich, S.; Goerigk, F. Effect of the damping function in dispersion corrected density functional theory. *J. Comput. Chem.* **2011**, *32*, 1456–1465.
- (43) (a) Dunning, T. H. Gaussian basis sets for use in correlated molecular calculations. I. The atoms boron through neon and hydrogen. *J. Chem. Phys.* **1989**, *90*, 1007–1023. (b) Woon, D. E.; Dunning, T. H. Gaussian basis sets for use in correlated molecular calculations. III. The atoms aluminum through argon. *J. Chem. Phys.* **1993**, *98*, 1358–1371.
- (44) Figgen, D.; Peterson, K. A.; Dolg, M.; Stoll, H. Energy-consistent pseudopotentials and correlation consistent basis sets for the 5d elements Hf–Pt. *J. Chem. Phys.* **2009**, *130*, No. 164108.
- (45) Pritchard, B. P.; Altarawy, D.; Didier, B.; Gibson, T. D.; Windus, T. L. New Basis Set Exchange: An Open, Up-to-date Resource for the Molecular Sciences Community. *J. Chem. Inf. Model.* **2019**, *59*, 4814–4820.